

# WGN

32:4  
august 2004

Visual perception  
Orbit calculation  
June Boötids  
Historical notes



ISSN 1016-3115

## Administrative

- Editorial *C. Trayner* 95
- Letters *A. McBeath* 96

## Ongoing meteor work

- A human visual perception model and its impact on Population Index estimation, ZHR, and best look direction *P.S. Gural* 97
- A spreadsheet that calculates meteor orbits *M. Langbroek* 109
- SPA Meteor Section Results: January-March 2002 *A. McBeath* 111

## Boötids

- 2004 June Boötids: video images and low-resolution spectra of 7P/Pons-Winnecke debris *P. Jenniskens* 114

## History

- Meteor Beliefs Project: The Palladium in ancient and early Medieval sources *A. McBeath & A.D. Gheorghe* 117
- The daylight meteor of 1866 June 20 *C. Trayner* 122

## Front cover photo

Romke Schievink with his video equipment at Britzingen, SW Germany (40 km north of Basel), shortly before the start of observations on 2004 August 11 at 20<sup>h</sup>15<sup>m</sup> UT.

## Future covers

Have you an interesting or spectacular meteor photograph that you think would look good on the cover of WGN? If so, please offer it to us. For the moment we can only accept machine-readable forms. More or less any image format will do, though ideally not JPEG as the JPEG compression algorithms lose information. A brief description will also be required: this should say what the photograph shows, when and where it was taken, plus (if possible) technical details such as the camera and exposure. We can be contacted at [wgn@imo.net](mailto:wgn@imo.net), but remember to put 'Meteor' in the subject line to get round the anti-spam filters.

**Writing for WGN** This Journal welcomes papers submitted for publication. All papers are reviewed for scientific content, and edited for English and style. Instructions for authors can be found in WGN **31:4**, 124–128, and at <http://www.imo.net/articles/writingforwgn.pdf>.

## Cover design Rainer Arlt

**Copyright** It is the aim of WGN to increase the spread of scientific information, not to restrict it. When material is submitted to WGN for publication, this is taken as indicating that the author(s) grant(s) permission for WGN and the IMO to publish this material any number of times, in any format(s), without payment. This permission is taken as covering rights to reproduce both the content of the material and its form and appearance, including images and typesetting. Formats include paper, CD-ROM and the world-wide web. Other than these conditions, all rights remain with the author(s).

When material is submitted for publication, this is also taken as indicating that the author(s) claim(s) the right to grant the permissions described above.

## Editorial — electronic publication

*Chris Trayner*

One of the purposes of the IMO is to publish. We publish WGN, IMC Proceedings, observation reports, handbooks and various other items such as shower calendars.

Most of these are published on paper, although there is some publication in electronic media. For instance the VMDB (Visual Meteor DataBase) is online on our website, <http://www.imo.net/visual/vmdb.html>. We also allow NASA ADS (<http://adswww.harvard.edu/>) to put WGN online. The intention is that issues will go online one to two years after publication, though at the moment there is nothing more recent than the end of 2000 (volume 28).

Publication on paper is convenient when many copies are made at once; it is less cost-effective when a small number must be produced. We are now faced with this situation, as the IMC Conference Proceedings for 1997 and 2001 are out of print. To reprint these on paper would be too expensive in money and time.

An alternative exists in the form of electronic publication, specifically on CD-ROM. When Mihaela Triglav-Čekada edited the IMC 2001 Proceedings, she produced a PDF (Adobe Acrobat) file of every paper. It is easy to put these together on a CD and make it available: we are now doing this with the 2001 Proceedings. Details can be found inside the back cover.

This venture is an experiment. In the light of experience we may continue it or abandon it. We may also have to change the price.

I would be interested to receive Letters to the Editor with your opinions on electronic publication. Would you prefer to have conference proceedings on paper or CD? Would you like to buy each year's WGN on CD so you can get rid of the paper? Would you prefer to receive WGN over the internet? This would be impossible at the moment, as it would require more work in Germany, and the WGN team there are already badly overloaded. But the only safe prediction about the future is that it will be different from the present, and the Letters page of a Journal is one way that an organisation works out where it wants to go.

## New Professional-Amateur Registry

*Communicated by Peter Jenniskens*

At the June meeting of the American Astronomical Society in Denver, Colorado, the AAS Working Group for Professional-Amateur Collaboration announced the inauguration of an on-line registry. This will be a searchable database that allows amateur astronomers to detail their abilities and professional astronomers to make known their observational needs.

At the moment, the registry is still being developed at <http://www.aas.org/wgpac/registry/> but is open to entries. Meteor observers interested in participating in professional observing campaigns with video, photographic, or telescopic (CCD) capabilities are encouraged to register.

*Peter Jenniskens is Chair of the Pro-Amat Working Group of IAU C22. For details, see WGN 31:5, 166–168.*

## Gnomonic Atlas Brno out of stock

The Gnomonic Atlas Brno by Vladimír Znovil is a standard tool for meteor observers. Unfortunately, we are informed that it is now out of print. If it is reprinted, we will inform you.

## Letters

### Not blinded by the light — Frederick Brodie's observations were accurate

*From Alastair McBeath*<sup>1</sup>

Chris Trayner's editorials in WGN continue to raise some interesting points. That in WGN **32:3** (p. 65), concerning the report of a possible superbolide seen crossing a fragment of the solar disc on 1864 October 1 by Frederick Brodie in southern England, caught my attention.

To answer a couple of queries Chris raised, his sketch image was correctly labelled by Brodie (that is, with 'south' at the top and 'west' to the left edge), assuming he was making a direct observation of the Sun through a typical inverting astronomical telescope. Brodie's use of a dark glass wedge reinforces this idea. Although nobody would suggest using such a solar viewing method modernly, this was a common practice in the 19th century. Filters for safe direct solar observing need to have been rigorously tested to ensure they cut down both visible and infrared radiation, sufficiently that the eye will not be irreparably damaged in using them thus.

Brodie also gave the time accurately as 22<sup>h</sup>30<sup>m</sup> GMT, since up to 1925, astronomers reckoned Greenwich Mean Time, GMT, from noon not midnight. This usage is now virtually obsolete, and has been retitled GMAT, Greenwich Mean Astronomical Time, to separate it from 'ordinary' GMT. Since 1928, at the recommendation of the IAU, GMT has been scientifically referred to commonly as UT or, now, UTC. The sighting Brodie made was thus at 10<sup>h</sup>30<sup>m</sup> UT, a more acceptable time for solar observing. Details on both the solar disc orientation and GMT/GMAT aspects can be found in the amateur astronomer's 'bible', Norton's 2000.0: Star Atlas and Reference Handbook (ed. I. Ridpath, Longman Scientific & Technical, 1989, pp. 57, 82 and 85). For all it seems modernly ludicrous the time system could ever have sensibly operated any other way, the change of GMT to GMAT, decided in 1917, but not put into practice finally until eight years later, was not without controversy, see for instance the comments and complaints recorded on p. 35 of *The History of the British Astronomical Association: The First Fifty Years* (ed. H. L. Kelly, BAA, 1948).

In regard to moving ripples in solar haloes, these have featured in WGN several times before (see for example my own notes in **21:3** (1993), p. 86, **22:4** (1994), pp. 134–136, and **25:2** (1997), pp. 108–114, esp. 113), and the complete list of such sightings is now maintained by the German *AKM* halo observing section (see website [www.meteoros.de](http://www.meteoros.de)). I was fortunate enough to have corresponded with, and met, Gunter Archenhold, who originated the theory these events might be due to sound waves propagated from meteors. Sadly he died in February 1999, aged 94. His father Friedrich was, among other things, an early pioneer of noctilucent cloud observing and photography in the late 19th century. The Archenhold Observatory in former East Berlin is named after him. It houses the massive Great Treptow refractor, with its 68 cm-diameter main lens, reputed to have the longest refractor tube in the world, and weighing ~ 120 tonnes!

Possible meteoric or asteroidal objects transiting the solar or lunar discs, but outside the Earth's atmosphere, have also been touched upon before in these pages, including in two of my articles on 'dark meteors' (WGN **23:3** (1995), pp. 91–96, and WGN **26:3** (1998), pp. 105–108). The second of these two papers also discussed a pair of modern sightings of intra-atmospheric meteors recorded crossing in front of the lunar disc. It would be interesting to know if there have been any modern recordings of meteors achieving a transit of the solar disc too.

<sup>1</sup> 12a Prior's Walk, Morpeth, Northumberland, NE61 2RF, England, UK. Email: [meteor@popastro.com](mailto:meteor@popastro.com)

# Ongoing meteor work

## A human visual perception model and its impact on Population Index estimation, ZHR, and best look direction

Peter S. Gural<sup>1</sup>

A meteor simulation tool with an improved human perception model is applied to address issues on population index estimation, ZHR correction, and best look direction for visual observers. The results indicate (1) the mean magnitude algorithm for estimating  $r$ -factor is robust to various shower and observing characteristics but one should use the new conversion formulae included herein, (2) the ZHR geometric correction related to the cosine of the zenith angle is not robust to the observer's look direction or meteor layer thickness, and (3) the guidelines for observing fifty degrees up in elevation from the horizon and within thirty degrees in azimuth from a radiant are found to be a sound recommendation for good counting statistics.

Received 2004 August 9

### 1 Introduction

A common question asked by new visual meteor enthusiasts is where in the sky they should direct their gaze when observing meteors. When the author first starting out in meteor observing during the 1970's, the recommendation was to observe  $45^\circ$  in elevation from the horizon and  $45^\circ$  off in azimuth on either side of the radiant you were most interested in that night. The latest IMO monograph edited by Rendtel et al. (1995) suggests that observers should look  $50^\circ$  to  $70^\circ$  up in elevation and from  $20^\circ$  to  $40^\circ$  off in azimuth from the radiant, never directing their gaze at the radiant. The arguments for doing so are usually made in an ad hoc fashion and invoke the notion that the longer trail lengths of meteors seen further from the radiant are more readily detectable as they trace greater angle swathes in the sky. The flip side favoring closer to the radiant are the reduced smearing effects of the meteor brightness over foreshortened path lengths thus making a given meteor seem brighter and thus more detectable. The path length argument tends to win out especially when one is interested in plotting meteors and a longer trail length makes plotting accuracies better and subsequent radiant association more robust. But issues that have not been clearly addressed are whether the combination of human perception and look direction have an influence on the science gathered by these observations. That is, are the observing recommendations and formulations used in data reduction valid for estimating meteoroid stream properties from visual measurements?

Motivation to investigate these issues derived from the author's earlier work on determining the best pointing direction for video meteor cameras. Using a meteor flux simulation code developed for intensified CCDs with moderate fields of view, Gural and Jenniskens (2000) showed that directing an imaging sensor towards the radiant would produce significantly higher counts. That paper also showed that flying at high altitude, where extinction is not a factor, leads one to maximize flux counts by pointing one's CCD sensor near

the horizon. However, human visual perception is more complicated and difficult to model than a CCD camera. Humans have a sophisticated image processor built into their visual cortex that is: (1) specifically tuned for motion detection and (2) not well modeled in terms of an analytic function due to the limited number of studies dealing with night vision. Would a radiant-centric observing direction for visual observers give enhanced counting statistics and what impact would it have on estimating population indices? To answer this question a meteor flux simulation tool was upgraded to include a realistic human perception model that closely matched the performance of a visual meteor observer. Thus one could examine issues in both meteor data collection and data reduction in a controlled fashion not subject to the vagaries of individual perception.

### 2 Meteor simulation

The first work on computer simulations of meteors was published by Van de Veen (1986a,b) and included a simple cosine model for perception and generated a table of population index versus mean magnitude. Results from that early work gave insights into population index estimation through analytic solutions and Monte Carlo simulations. For the current work, a higher fidelity model of perception is used and greater sophistication in the geometric effects influencing the visibility of meteors is included. Note that the author made a first attempt at this form of analysis in (Gural, 2003) but the use of a higher fidelity set of models in this paper renders the results from that earlier work obsolete. However, the use of random trials on a computer to obtain the overall statistical behavior remains the fundamental tenant that is common to this and the previous studies.

The software simulation used for this task was a program developed by the author entitled METEORSIM that is described in greater detail in (Gural, 2001). To summarize, METEORSIM is a C language program that takes a uniformly-distributed random spatial distribution of particles with a given population index and propagates each particle relative to a specified radiant direction in space. During the Monte Carlo processing each particle is (1) propagated with uniform velocity under

<sup>1</sup>351 Samantha Drive, Sterling, Virginia, USA 20164.  
Email: peter.s.gural@saic.com

the influence of zenith attraction, (2) tested for intersection with the Earth's atmosphere at a user specified begin and end height, (3) tested for line of sight above the observer's horizon, (4) have a random absolute magnitude drawn from a specified population index distribution, (5) have each particle's magnitude corrected for distance fading, extinction, and angular velocity losses, and finally (6) tested to be above a limiting magnitude and perception probability, the last having at least a functional dependence on the elongation angle relative to the observer's staring direction. The angular velocity loss and off-axis perception are two areas where the modeling was recently upgraded for human observers (for CCD modeling a unity perception is assumed across the field of view and the loss terms were strictly proportional to the time a meteor dwells within a pixel).

Three functional capabilities were added to the software to obtain (1) statistics of the effective observed perception given the implemented model in the code, (2) magnitude distributions and counting statistics for a single look direction, and (3) flux data for look directions covering the entire sky. Typically one billion meteors were simulated to obtain good counting statistics of several thousand for a given look direction. This took from an hour to several days of processing on a 1.7 GHz Pentium IV PC depending on the mode selected.

For the baseline meteor stream parameters, the Perseids were chosen to represent an average shower and also to more closely match the characteristics under which the perception model measurements were based. The baseline was thus set at a population index of  $r = 2.6$ , begin height of 114 km, end height of 94 km, entry velocity of 59 km/sec, radiant in the east at an azimuth of  $+90^\circ$  and radiant elevation at  $+45^\circ$ . The baseline observing direction was at an azimuth of  $+60^\circ$  ( $30^\circ$  off in azimuth from the radiant) and look elevation of  $+50^\circ$ . Deviations from this nominal case will be discussed in later sections.

### 3 Human perception modeling

The human visual system is highly adept at detecting faint meteors in its foveal (central) field and is known to lose sensitivity as the elongation angle of the meteor off the look direction increases. In addition, the visual cortex has been found to be variably adept at detecting moving objects both on and off axis and is a modeling characteristic that is required to properly account for human visual acuity of meteors. The latter characteristic can be modeled through a correction of the magnitude of the meteor as a function of its apparent angular velocity as seen from the perspective of the observer. The model used was based on the work of Hoffmeister (1948) where the results of his studies have been plotted in Figure 1. Below the maximum angular rate of  $51.5^\circ/\text{s}$  for non-hyperbolic meteors, the magnitude gain/loss can be approximated by a linear function which produces brighter meteors (negative value of correction) for slower angular velocities. Note that the maximum angle rate was computed for a maximum entry velocity of 72 km/sec, minimum meteor distance of

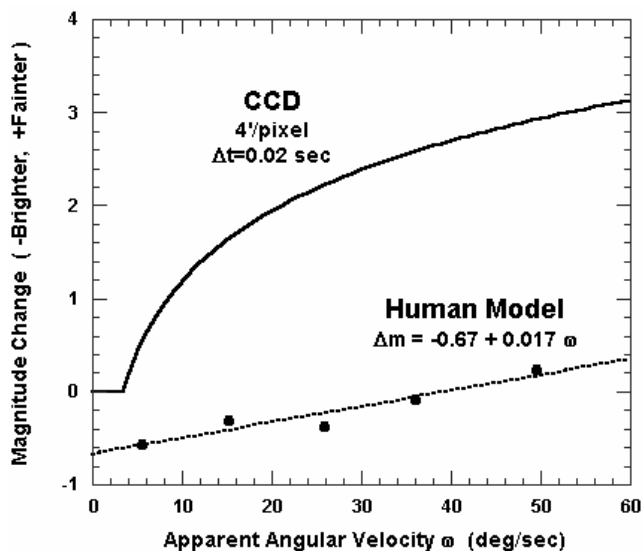


Figure 1 – Magnitude gain (–) or loss (+) of a meteor relative to its absolute magnitude as a function of its apparent angular velocity. Shown are human measurements (closed circles), model fit (dotted), and CCD (solid) response curves.

80 km, meteor observed in the zenith and the radiant at the horizon. When running a simulation, one knows the apparent angular velocity of each meteor from geometry and its shower parameters, and thus the magnitude loss can be easily applied. Note that in Figure 1 the angular velocity loss of a CCD chip shows a far steeper magnitude change with greatly enhanced detection capability for slower moving meteors. This characteristic of video cameras is the reason for the higher counting statistics when pointing a CCD sensor near the radiant where meteors have low angular rates of motion. The flatter behavior of the human visual system is the first indication that such an advantage will not be as great for visual observers.

More significant in proper modeling of the human visual system is the effect of off-axis perception as a function of magnitude and elongation angle. Work done on characterizing the probability of perception for visual observers by Koschack and Rendtel (1990a,b) was used to form the basis of the model used in the current METEORSIM simulation. These two authors have documented the data reduction of five visual observers whose measurements had been collected during the months of July and August around the time of the Perseids. The data collected from the observers over several nights had been smoothed and combined into a single table of perception versus elongation angle  $R$  and magnitude distance  $\Delta m$  from the limiting magnitude. For this paper, an analytic model was developed to mimic the characteristics of that data set with the details of the functional form given in Appendix A. Figure 2 shows the comparison of the model to the published perception data showing a high level of consistency between the two. The model does accurately portray the perception across a large range of magnitudes and elongation angles and deviates from the smoothed data in regions of low perception and little consequence. It should be noted that the raw data from the individual observers

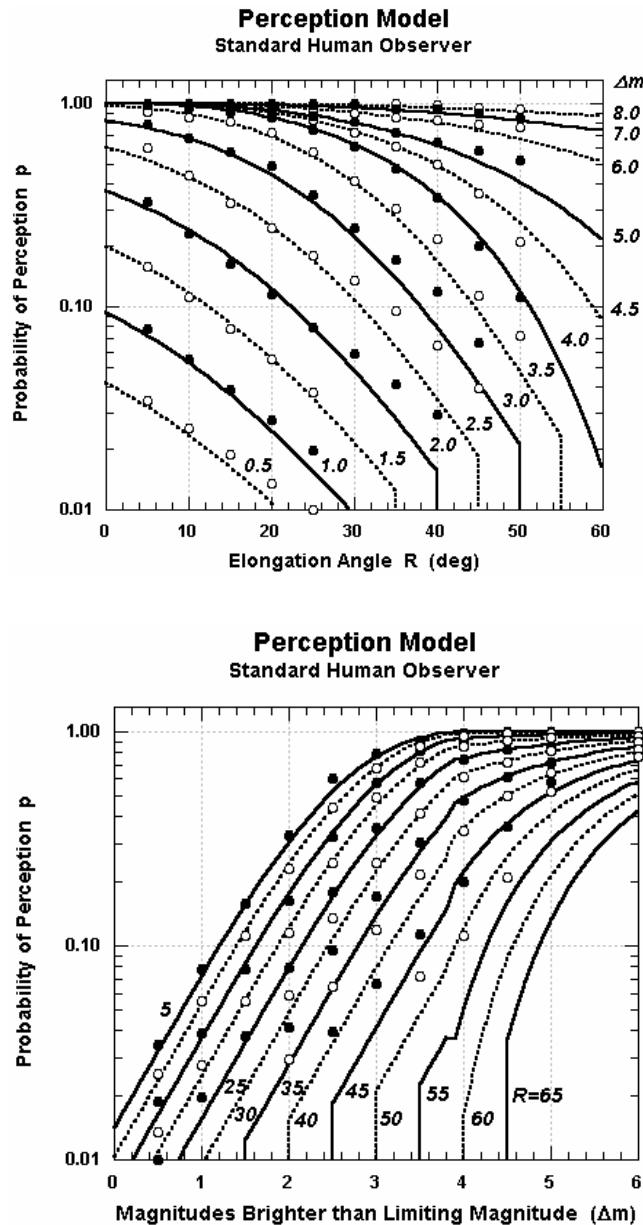


Figure 2 – Perception as a function of elongation angle for fixed magnitude shifts (top) and as a function of magnitude shift for fixed elongations (bottom). Smoothed data (circles) from Table 4 of (Koschack & Rendtel, 1990a) and the HPM90 analytic model (solid lines).

shows a wide variance in perception and this model fits well within that spread. For the remainder of this paper, the analytic model used herein will be referred to as the Human Perception Model 1990 (HPM90) as it is based on the tabulated data in Koschack and Rendtel (1990a,b) and will be taken as representative of a standard visual observer.

In a simulation, the population index and shower parameters are known, the counting statistics are high, and the perception gets applied in a consistent and known fashion. Thus studies in population index estimation, ZHR correction, and flux rates can be done in a controlled environment. For example, the average perception as a function of elongation angle only can be obtained directly by comparing meteors detected with the total known meteors that could have been found

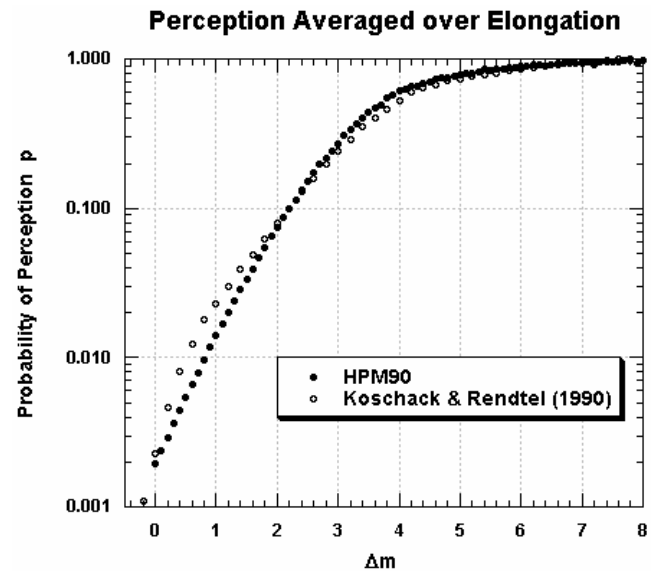


Figure 3 – Perception averaged over the elongation angles of 0 to 52.5° plotted as a function of  $\Delta m$ .

— outputs easily obtained in the simulation. This contrasts with the approach used in (Koschack & Rendtel, 1990a,b) where they needed to make computations for surface area and corrections for distance. In Figure 3 is shown the average perception function of the two methods showing a high degree of correlation despite the different approaches used to arrive at the answer. The analytic expressions that fit these curves are included in Appendix A. We will however, concentrate on the HPM90 model to examine the methods employed to correct counts when estimating the population index.

#### 4 Population Index estimation via cumulative counts

The mathematical definition of population index is the ratio of the integrated numbers of meteors brighter than magnitude  $m + 1$  to the integrated numbers of meteors brighter than magnitude  $m$  (important note: in the limit of high counting statistics this can be well approximated by the ratio of counts of meteors in magnitude bin  $m + 1$  to the counts in magnitude bin  $m$ ). Thus it was commonplace until the late 1990s to obtain a magnitude distribution from an observation, correct to the true counts per magnitude bin using the average perception function of Koschack and Rendtel (1990, Table 15), form the cumulative counts as a function of  $m$ , and finally fit with a power law function to find the underlying population index  $r$  of the meteor stream. Regions of low counts (typically negative magnitudes) and rapid perception falloff (within two magnitudes of the limiting magnitude) are typically avoided in applying the fit. Given that the simulation has a very well determined perception function and excellent counting statistics, this method was applied to a baseline simulated Perseid parameter data set but found not to be a reliable estimator of  $r$ .

To identify the various sources of counting errors that could cause the poor performance, one must first examine the behavior of the simulated data. As seen in

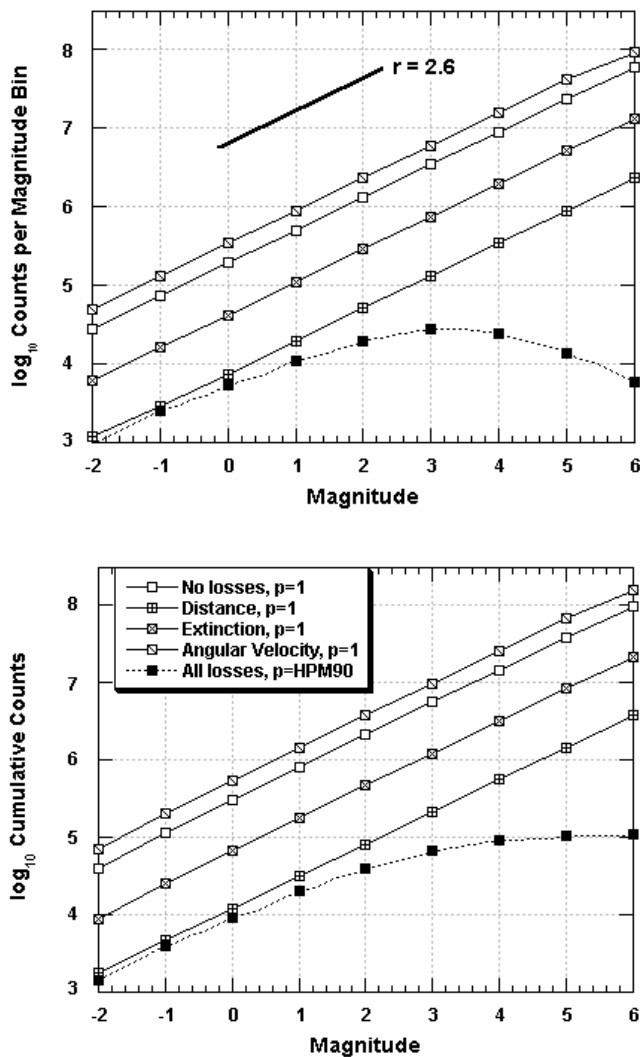


Figure 4 – Magnitude distribution (top) and cumulative counts (bottom) as a function of magnitude for the baseline simulated Perseid shower parameters. The  $lm=+6.5$  and a population index of  $r = 2.6$  was used which yields a slope of 0.414 per magnitude.

Figure 4, the geometric and environmental influences on count statistics such as distance fading, extinction, and angular velocity losses do not affect the slope of the line of cumulative counts versus magnitude when the perception is unity over the field of view. For example, the visual angular velocity model induces a gain in counts (effective shift in limiting magnitude), whereas the distance losses cause the greatest decrease in counts followed by the extinction losses. But the slope of the counts versus magnitude remains fixed at the baseline  $r$ -factor of 2.6. Note however, that when the human perception elongation sensitivity is included, the counts deviate significantly from a simple power law function (i.e. the counts deviate from a linear function in the semi-log space that has been plotted). It is quite evident in Figure 4 when the HPM90 model has been used for the perception, there is no range of magnitudes where (1) there are sufficient count statistics and (2) the visual observer's counts show a power law trend (linear line segment) covering several magnitude bins.

Herein lies the reason for the attempt to correct the counts beforehand to obtain the true slope and thus the

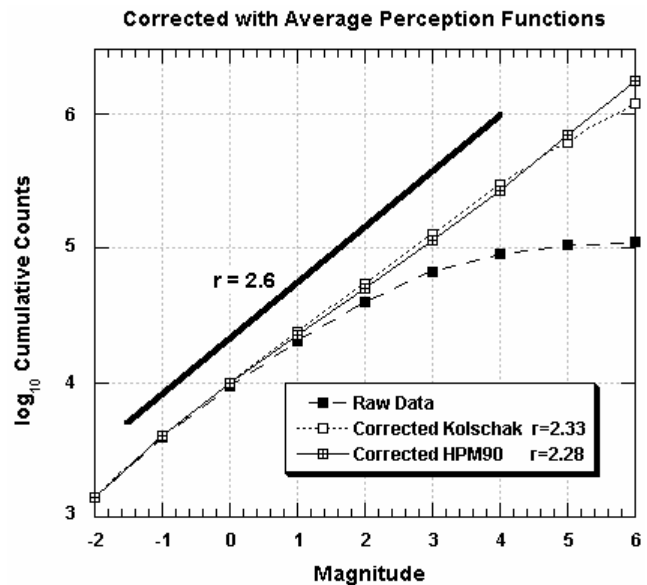


Figure 5 – Cumulative counts versus magnitude when corrected with the average perception functions of (Koschack & Rendtel, 1990a) and HPM90.

population index. Until recently this was done by dividing the cumulative counts by the average perception function. The average perception as a function of a single variable  $\Delta m$  was used since observers typically do not record the elongation of the meteor or its altitude above the horizon and therefore this simplifies the data collection and reduction. In Figure 5 is shown the result of having corrected the simulated counts with the two average perception functions of Figure 3. In the case of using the HPM90 model, one would have expected the best possible result since its average perception function is self consistent with the data simulated. However, note that when either model is used, the estimate for the population index between magnitudes +0 and +4 is underestimated by 0.3. Please note that this magnitude range is typically used in data reduction and the slope estimated via LMS linear fit as it has the highest level of counts. Attempts at other population indices ranging from 1.5 to 4.5 found that the fit to the slope also produced a typical underestimate of three tenths from the true value of  $r$ . In a more extreme deviation from the baseline, using a simulated population index of  $r = 3.6$ , entry velocity of 25 km/sec, and radiant elevation of  $70^\circ$ , the underestimate amounted to four tenths. Thus even in a controlled situation with high counting statistics and accurately known perception function, the cumulative counting methodology of population index estimation runs into difficulty when based on average perception versus  $\Delta m$ .

## 5 Population Index estimation via mean meteor magnitude

Since the late 1990s, the IMO has adopted an alternative method of estimating population index that was discussed by Kresakova (1966), computer generated by Van de Veen (1986b), and has been recomputed and applied by Arlt & Gyssens (2000) and Arlt (2003) to obtain  $r$  for the recent Leonid storms. Each author has

presented a conversion table that maps the average meteor magnitude directly to the population index of the meteors. The method is elegant in its simplicity but sensitive to the fidelity of the perception model employed. Discussions with Arlt (2004) indicate his most recently published table was generated by computing the first moment of the magnitude distance (mean  $\Delta m$ ) using as a weighting function ‘the product of the average perception function  $p(\Delta m)$  of (Koschack & Rendtel, 1990b, Table 15) and the probability the meteor will be a particular magnitude above the limiting magnitude’. This is reproduced in equation (1).

$$\langle \Delta m \rangle = \frac{\sum \delta m \cdot p(\delta m) r^{-\delta m}}{\sum p(\delta m) r^{-\delta m}} \quad (1)$$

such that  $\delta m = [0, 14.5]$

The fundamental idea behind the approach is depicted in Figure 6, where magnitude distributions collected by a simulated visual observer (HPM90) show a drift in the peak counts away from the limiting magnitude of +6.5 as  $r$  decreases. This is because the larger numbers of brighter meteors in proportion to the fainter particles are more readily visible at the larger elongations, which is more detectable for visual observers. This pushes the ‘hump’ to the left in Figure 6 and lowers the mean magnitude to a brighter value. The conjecture is that a simply computed figure of merit such as the difference between the mean magnitude and the limiting magnitude ( $\Delta m = \text{lm} - \langle m \rangle$ ) is uniquely determined for each population index and unvarying with observing conditions. This also assumes that the population index is constant over the range of magnitudes that contribute significantly to the mean. Please note that an issue arises when the population index becomes small ( $r < 2.0$ ) and the number of meteors in magnitude classes brighter than  $-8$  begin to significantly affect the mean. The correct mean normally would include all magnitude classes with significant counts. However, when applying the conversion only those magnitude classes with  $\Delta m < 14.5$  should be used since the tables in Appendix A were generated with this cutoff in the statistical calculations (e.g. use up to magnitude class  $-8$  for  $\text{lm} = +6.5$ ).

For the METEORSIM simulation it was a simple matter to run through a range of population indices and obtain the mean magnitude for each case using the HPM90 model, the baseline observing/shower conditions, and several billion simulated meteors. The comparison of the previously published table of Arlt (2003) and the simulated results generated herein is displayed in Figure 7 (the values and analytic fit to the HPM90 model data can be found in Appendix A). In general the Arlt table, based on the average perception function of Koschack, again underestimates the population index by 0.3 to 0.5. It is interesting to note that this is the same order of underestimation that occurs when using the cumulative counts approach to  $r$  estimation, which was coincidentally corrected with the same average perception function. Since the new conversion table is derived from a more general two-parameter model of the

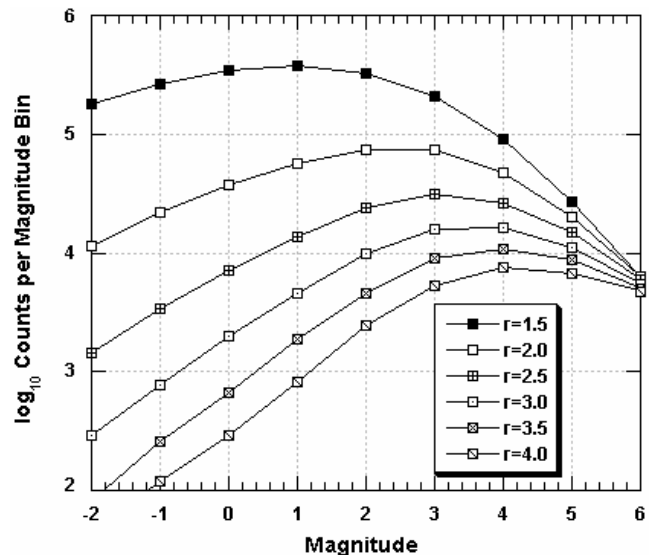


Figure 6 – Magnitude distributions for simulated meteors with various population indices and the HPM90 perception model. These are based on a limiting magnitude of +6.5.

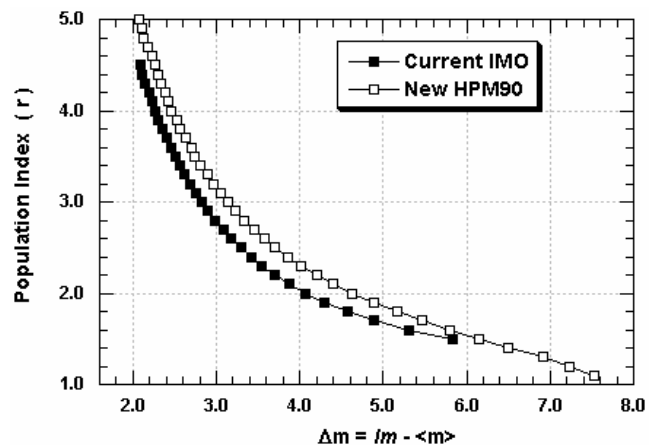


Figure 7 – Population index as a function of mean magnitude distance from the limiting magnitude.

perception and coupled to the three-dimensional effects of geometry and loss, it is recommended that this new result should be used in all future data reduction work (until such time that a more improved perception model is developed). In Appendix A will be found the revised conversion table that is based on the HPM90 standard observer as both tabulated numbers and in the form of an analytical functional fit.

Since the mean magnitude approach has now been calibrated for the baseline scenario of observing conditions, geometry, and the HPM90 standard observer, the next step is to verify its robustness to deviations from the baseline. For input population indices of 1.5, 2.0, 2.5, 3.0, 3.5, and 4.0, each of six different parameters were varied from the baseline shower settings over realizable limits to determine the impact on estimated  $r$ -factors. A mean magnitude was generated and mapped back to  $r$  via equation A-4 in the appendix and plotted in Figures 8 and 9 versus radiant elevation, entry velocity, begin/end height, look azimuth, look elevation, and observer altitude. The latter case effectively involves a reduction in extinction near the horizon. The resul-

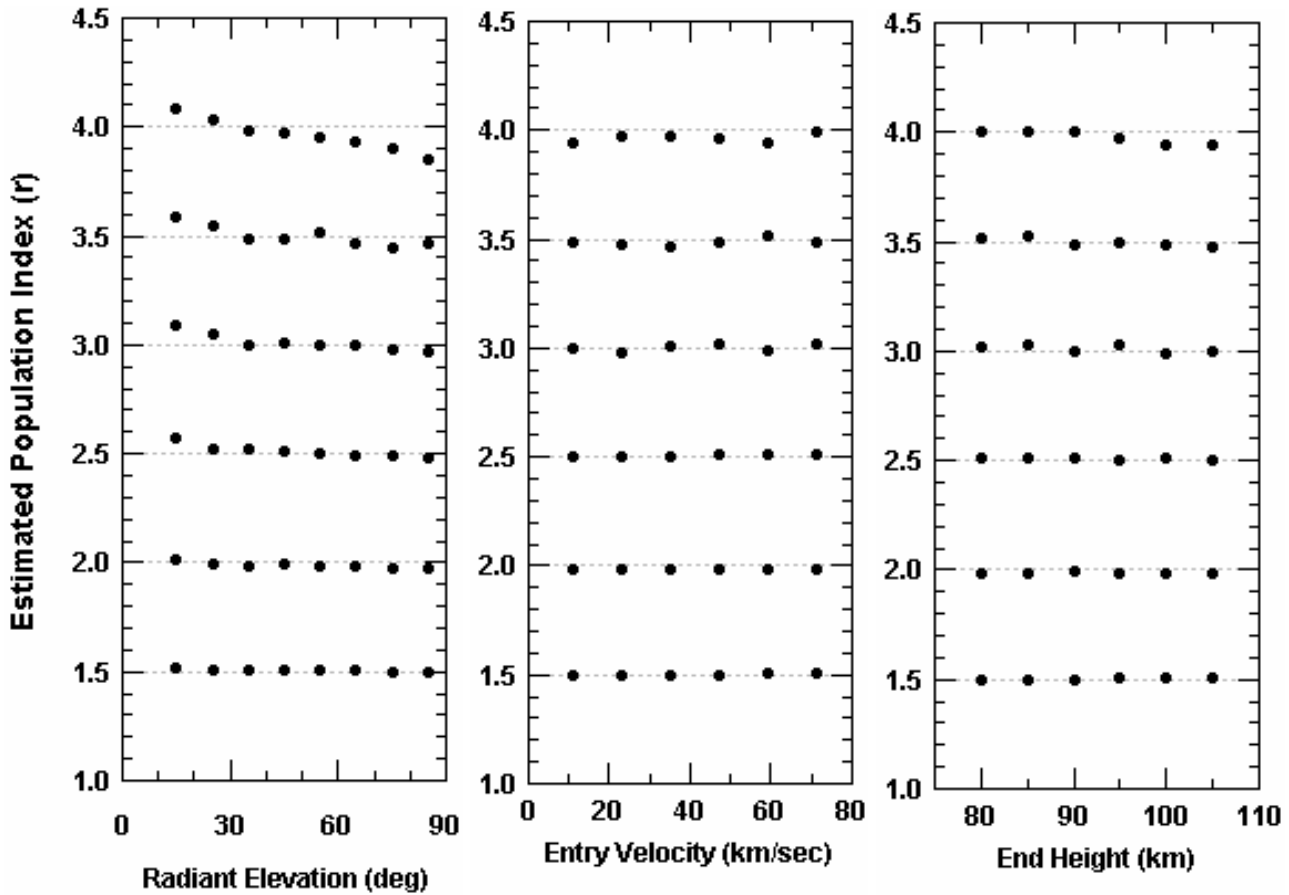


Figure 8 – Population index estimation for variations from the baseline scenario in radiant elevation, entry velocity, and end height (begin height = end height + 20km).

tant findings show that the mean magnitude method is very robust to most of these parameter changes as evidenced by the flat response of the circular points in the figures. Note that the gray horizontal lines represent the true population index and the plotted points are the estimated values. Typically, for a large variety of the parameters that were changed, the population falls within one-tenth of the true value. The one exception is in the variation with the observer's look elevation above of the horizon. At  $50^\circ$ , where the HPM90 conversion formula of equation A-4 was calibrated, the estimate is very good. For other look elevations, deviations of greater than one-tenth in  $r$  are evident in the plots, and is the first reason for not observing at higher or lower elevation angles (the second reason that will be discussed later is for maximizing counting statistics). The other somewhat problematic area is when the population index is high and the radiant elevation is varied. High population indices are harder to estimate because a small variation in the mean magnitude induces a large change in  $r$ . The conversion formula was calibrated for foveal vision at a radiant elevation of  $45^\circ$  and thus performs best there but clearly could be improved for other elevations. As will be seen shortly, the errors associated with limited counting statistics overwhelm these mis-estimations. In general then, the method of mean magnitude  $r$  estimation can be applied confidently for most any observing conditions encountered.

The last item to consider before leaving the topic of

population index estimation is what standard deviation can be expected in  $r$  given that the counting statistics are usually quite small, the magnitudes are discretely binned in steps of unit magnitudes, and the magnitudes are estimated with an error of as much as a half magnitude. Arlt (2003) presented a similar result showing strictly the impact of number of counts versus population index. This analysis follows a similar methodology via a statistical estimate of the standard deviation in  $r$  where the total counts observed were fixed over many Monte Carlo trials. It was found that discretization into unit sized magnitude bins and having an unbiased uniform magnitude estimation error of one-half magnitude were relatively small contributors (less than 5%) to the total standard deviation of the population index estimate as compared to simply the impact of low counting statistics. The standard deviation in  $r$  was found to decrease inversely proportional to the square root of the number of meteors used to form the mean magnitude estimate — as one would intuitively have guessed. A typical value of  $\sigma_r = 0.014$  is found for  $r = 2.6$  and 100 meteors and grows larger for increasing population index. A generalized formula given arbitrary population index and meteor counts, is given as expression A-5 in the Appendix.

## 6 Zenith Hourly Rate

The corrections for zenith hourly rate (ZHR) for human visual observations include adjustments for the time pe-

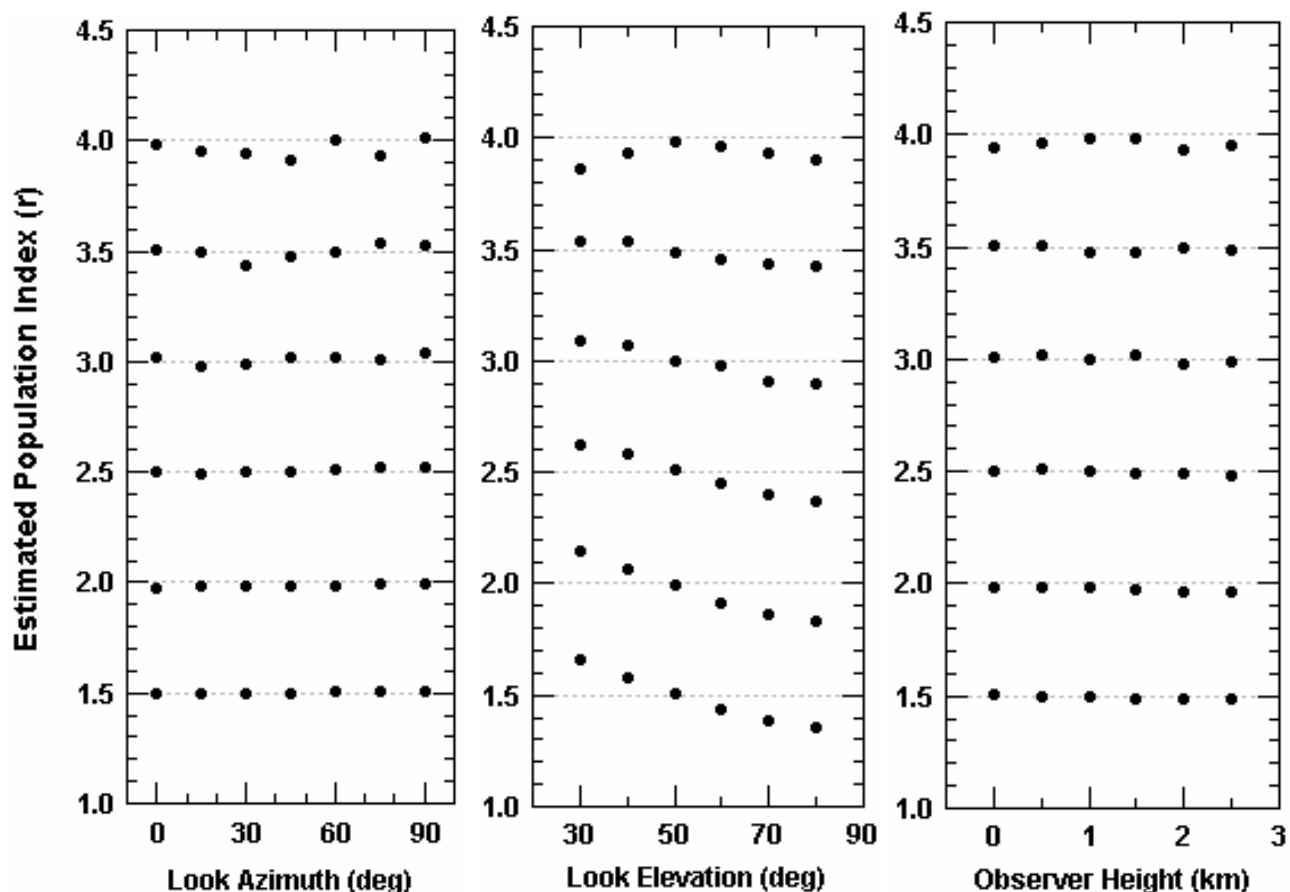


Figure 9 – Population index estimation for variations from the baseline scenario in look azimuth, look elevation, and observer altitude.

riod of observation, cloud obscuration, limiting magnitude, and zenith distance ‘ $z_a$ ’ of the radiant. Of these, the latter is the only geometric correction term between the radiant and the observer that has been considered in standard data reduction efforts. Employing the HPM90 model to examine meteor flux rates under variable meteor/observer geometries has indicated that the apparent angular velocity effects of off-radiant observations, the thickness of the meteor layer, and the look direction of the observer all significantly influence the ZHR estimation so that the  $\cos(z_a)$  correction is only weakly valid. Curiously, the perception model itself does not appear to affect the ZHR, but rather simple geometric effects come into play and thus may lead to more analytically robust correction formulae. This paper does not try to formulate these correction terms as this will require further study and analysis. It does try to point out the areas where deficiencies can arise and how in some circumstances one can minimize their influence by adhering to certain observational restrictions.

The finite thickness of the meteor layer, that is the separation between the average begin and end heights of a particular shower stream, and thus the meteor’s length can cause an overcorrection in the ZHR by as much as 25% when using  $\cos(z_a)$  as the correction term. This can be seen in Figure 10 where the radiant was repositioned through various elevation angles and the meteor flux simulated for various look direction azimuth offsets (from staring in the direction of radiant azimuth

to  $90^\circ$  away). Note that, for the cases run in Figure 10, the angular velocity loss has been removed to eliminate its deleterious influence on this stage of the analysis. Extinction and distance fading losses were included however. As can be seen in the plot at the top where the meteor layer thickness was essentially made infinitesimal (begin height equals end height), the observed counts follow the well-known  $\cos(z_a)$  curve almost exactly and independently of observer look direction. This excellent agreement is because the standard ZHR correction was derived assuming a very thin atmospheric cap in its formalism.

However, when the begin and end heights are set to the more realistic baseline case of 114 km and 94 km respectively, as depicted in the plot at the bottom of Figure 10, the measured meteor counts seriously deviate above the  $\cos(z_a)$  curve over a large range of radiant elevation angles. Thus if the counts were to be divided by the standard zenith angle correction term of  $\cos(z_a)$ , the result would be an overestimation in the ZHR for low to moderate radiant elevation angles.

A more detailed analysis shows this effect to be solely due to the length of the meteors manifested by their average begin and end heights, and thus it should be possible to derive a more representative correction term (in the absence of angular velocity losses) based on the volume intersected and projection of the meteor’s full track length. In fact, this may be one contributing factor for the need to use a non-unity power law on the

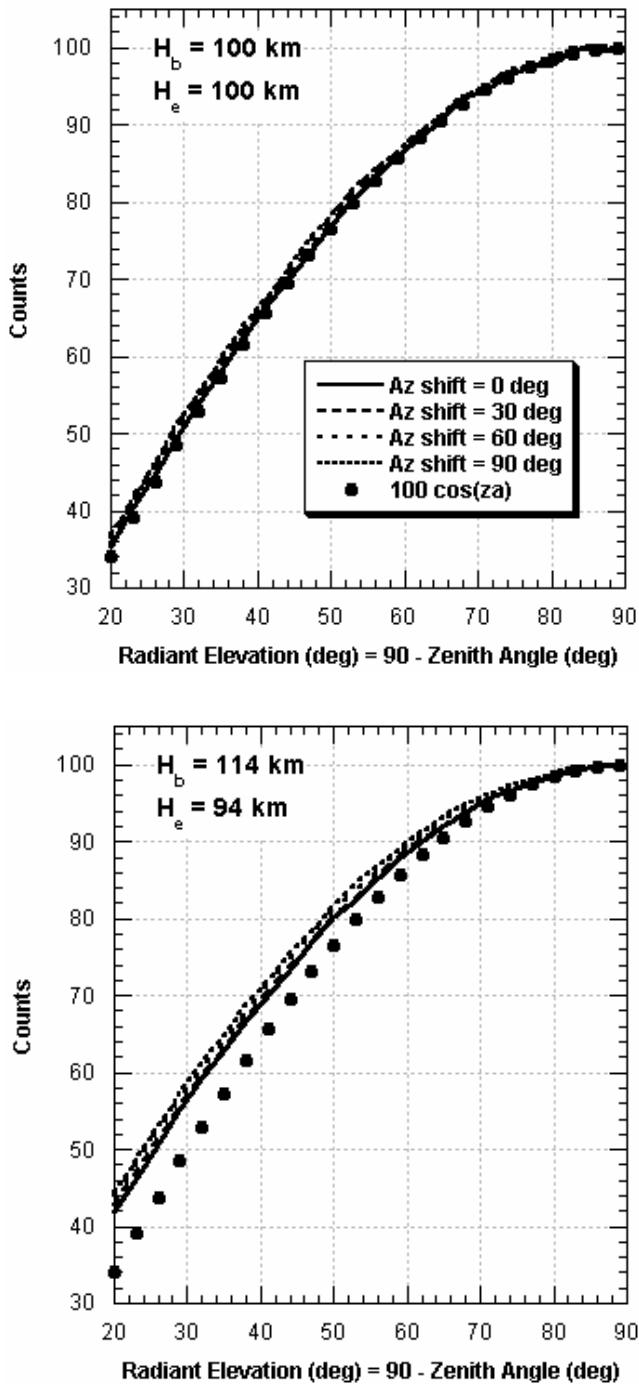


Figure 10 – Meteor counts as a function of radiant elevation angle above the horizon for various observer look directions relative to the radiant's azimuth. The plot at the top is for an infinitesimally thin meteor layer and at the bottom for the baseline begin and end heights of 114 km and 94 km.

cosine term, that is a  $\cos^\gamma(za)$  correction seen in papers published by Prentice (1953), Zvolankova (1982), and Bellot Rubio (1995). In the case of Figure 10 (bottom plot) the power that fits the simulated curves extremely well arises when  $\gamma = 0.8$ .

Note that, for the simulated meteors used herein, the gamma power is expected to be unity since the meteors are modeled with a brightness function that is independent of entry angle (dustball model) instead of the brightness being a function of the cosine of the zenith angle ( $\gamma = 2$  for solid bodies). Figure 10 (top) shows

that  $\gamma = 1$  was indeed found when the meteor length was not a factor and the dustball model is employed. Clearly then, the detectability of the long meteor trail enhances the count statistics (especially for lower radiant elevations) and should be accounted for when arguing between dustball and solid body physics. That is, the meteor length biases the interpretation towards dustball meteors when one is evaluating visual meteor observations.

Further analysis indicates that the human perception model used in this study was not a factor as the final result is the same when a perception function of unity is used over a finite field of view. In addition, the azimuth look direction of the observer does not cause variability in the counts as evidenced by the tightly overlapping curves in both plots of Figure 10 when there are no angular velocity losses.

The meteor count behavior becomes more complicated when the angular velocity loss terms are included. Now the relative geometry of observer look direction and radiant direction plays a significant role in the number of counts seen and an extreme variability in observed counts can occur simply by looking in different azimuth directions away from the radiant. This is clearly depicted in Figure 11 where the curves are no longer co-aligned and also do not follow the expected counts curve. In fact, one can see more meteors (but only marginally so by 2%) when the radiant is high but not at the zenith and the observer stares at the radiant. Applying the standard correction term of  $1/\cos(za)$  results in the curves of Figure 12 where overestimation of the ZHR can be seen for all observer look directions other than the case staring  $90^\circ$  from the radiant. That particular look direction actually appears to be consistent with the standard correction term down to a radiant elevation angle of  $40^\circ$ . Below that altitude the correction begins to fail for that geometry as well. Thus the immediate conclusion one draws from this Figure is that an observer should look far away from the radiant to properly correct to actual ZHRs. However, one should note that in the next section it is recommended from a statistical counting perspective that one should not look that far off the radiant lest they miss a third of the observable meteors. Thus the twin goals of maximizing meteor counts and minimizing the influence of angular velocity losses on ZHR mis-corrections appear to meet with conflicting requirements. It would seem at this time that the former goal should be emphasized for consistency with past data collection and a more robust correction formula derived to deal with the angular-velocity/look-direction ZHR issue. Note that any future corrections to remove this issue in ZHR analysis will require that observers record their look and radiant directions diligently in all future observing campaigns.

## 7 Best look direction

This last section deals with answering the question: what is the best look direction for visual meteor observers to maximize their counting statistics? As it turns out, not all look directions are equally good. For

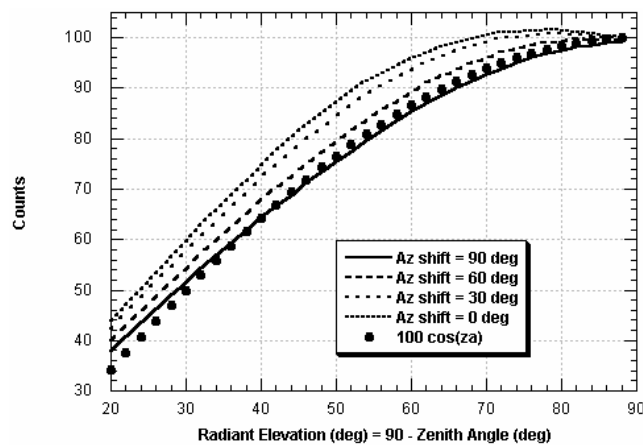


Figure 11 – HPM90 observed counts for different azimuth look directions relative to the radiant azimuth. The large dotted curve is the expected counts based on standard IMO correction factors for geometry.

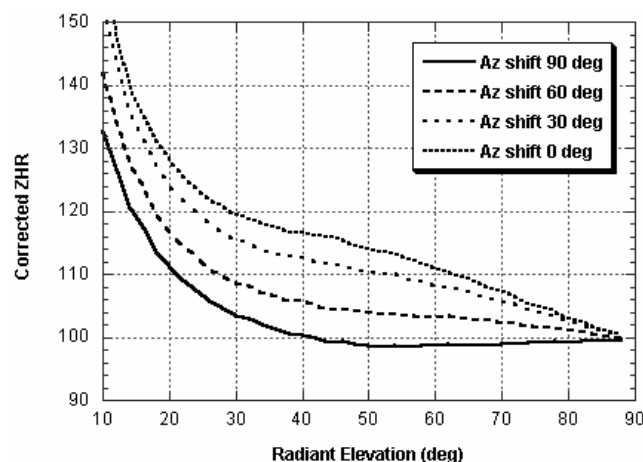


Figure 12 – ZHRs for counts in Figure 11 corrected via inverse of the cosine of the zenith angle for the radiant. Note there is an overcorrection of 10-20% for moderate radiant elevations. The true ZHR in this case should be 100.

example, it is obvious that staring down at a very low elevation direction towards the horizon is a poor choice due to the horizon/ground cutting off the observer's field of view and the increased magnitude losses associated with atmospheric extinction and distance fading (exception: when the  $r$ -factor is very small). Intuitively, looking at the zenith is also a poor choice due to the reduced volume of the meteor layer that the observer can discern (exception: when the radiant is also at the zenith). Using HPM90 within the meteor simulation and examining count statistics (normalized per square degree) for all look directions given a discrete set of radiant elevations every ten degrees resulted in the following set of observations:

1. For low elevation radiants and an  $r$ -factor of 2.5, to achieve 90% of maximum counts possible, one should observe between  $30^\circ$  and  $60^\circ$  elevation above the horizon and within  $45^\circ$  azimuth of the radiant's position. For radiants with higher elevation angles, the observable region grows upwards in elevation and outwards in azimuth.
2. For higher  $r$ -factor than 2.5, the observable sweet

spot decreases in size raising the minimum observable elevation to  $45^\circ$  and shrinks the maximum azimuth extent away from the radiant to  $\pm 30^\circ$ . For streams with a lower  $r$ -factor than 2.5, the sweet spot grows in azimuth from the radiant and the best observing elevation drops closer to the horizon with severe losses incurred for staring at the zenith.

3. Observing  $180^\circ$  around from the radiant (radiant towards your back) can incur counting losses of up to 50% from nominal.

In order to try and focus on a single best choice under a variety of observing conditions that may be encountered, one could examine the worse case counts by combining all the radiant elevation and population index results into a single plot. For each case of radiant elevation from  $20^\circ$  to  $90^\circ$  and population index of 1.8 to 3.8, a normalized flux count relative to the max counts achievable was obtained. These were then combined and presented as worse case flux contours in Figure 13. From the Figure it is evident that the best overall look direction for maximizing counts is  $50^\circ$  in elevation and  $\pm 30^\circ$  from the radiant's azimuth. Note that the radiant was set to an azimuth of  $90^\circ$  in all the cases depicted in this paper and thus the peak in Figure 13 is found between  $60^\circ$  and  $120^\circ$ . For other radiant azimuths the maximum simply rotates around to align with the radiant. Thus looking in the general direction of the radiant is highly recommended. Please note that the precise lack of symmetry in counts around the radiant's azimuth and the anti-radiant azimuth ( $90^\circ$  and  $270^\circ$  respectively) is simply due to the limited counting statistics of the Monte Carlo simulation process. From the Figure one would actually infer that the best elevation angle to look is closer to  $40^\circ$ . However, any given local site may have higher atmospheric extinction than that used in the METEORSIM modeling and, furthermore, there is an innate desire to avoid seeing the ground cutting off one's field of view, thus leading to a recommended elevation angle biased higher than  $40^\circ$ . Clearly, however, observing at elevation angles of  $60^\circ$  or more can result in a significant loss in total count statistics.

## 8 Conclusion

The following main points were presented in this paper:

- Using the average perception function in either the bin-count-correcting or the mean-magnitude methods of population index estimation results in an underestimate of the population index by at least 0.3.
- The mean magnitude method for population index estimation is found to be very robust to a variety of observing conditions.
- Recommend using the new conversion formula in equation A-4 to convert from mean magnitude to a population index estimate to more accurately account for human perception.

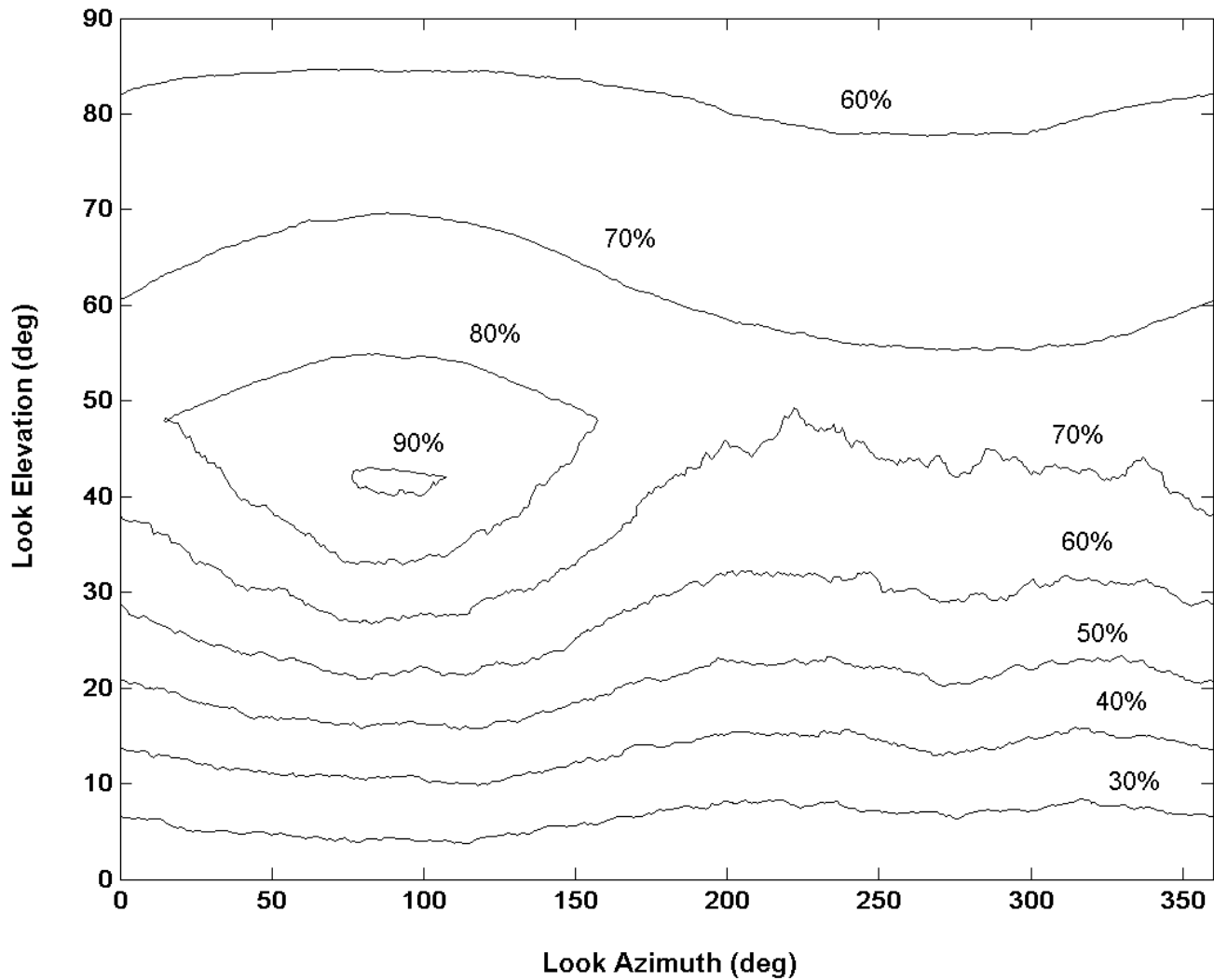


Figure 13 – Contour plot of the count percentage relative to the maximum possible. Results combined for various radiant elevation angles from  $20^\circ$  to  $90^\circ$  and population indices from 1.8 to 3.8 with the radiant located at an azimuth of  $90^\circ$ .

- The standard geometric correction of  $1/\cos(\text{za})$  overestimates ZHR by 10% or more depending on radiant elevation and look azimuth relative to the radiant direction. This is due to the finite meteor layer thickness and the angular velocity loss behavior of a human observer.
- The best look direction for a human observer is to observe at an elevation angle of  $50^\circ$  above the horizon and within  $30^\circ$  of the radiant's azimuth. Staring in alignment with the radiant's azimuth does not diminish total meteor counts given the angular velocity model used herein.

Future work that needs to be addressed includes the impact of higher fidelity light curve modeling on the results contained herein. Does the fact that the magnitude is lower at either end of the meteor trail length reduce the effective atmospheric cap thickness for a visual observer and thus return the ZHR correction term closer to the standard  $1/\cos(\text{za})$  factor? Is it possible to derive analytic expressions to account for the angular velocity loss given the observer's stare direction relative to the radiant? And lastly, can we further improve the standard observer perception model to more accurately represent

visual observations? A worthwhile project in this last area would involve the simultaneous collection of video observations with experienced human meteor observers. With a battery of intensified video cameras that reach to a meteor limiting magnitude of  $+6.5$  one would have 'truth' in terms of meteor magnitudes, positions, and angular velocities. The visual observations could then be compared with respect to the known data, deriving two dimensional perception functions and detection sensitivity to angular velocity. These could then be used in a refined HPM model for simulating and verifying the corrections one needs to apply to visual observations.

## Acknowledgments

This work was initially inspired during a recent Leonid campaign where the author had the pleasure to discuss best viewing conditions with long time visual observer, Robert Lunsford. Bob had instinctively felt that it was far better from a counting perspective to stare at the radiant in order to increase counts by up to 50%. Based on the results of this paper that the gain is only marginal when looking at the radiant, Bob may have uniquely better perception for slower meteors than standard ob-

servers. I would also like to thank Stephen Schiff for providing an English translation of Hoffmeister's (1948) key work in angular velocity losses with respect to human perception of meteors.

## References

- Arlt R. (2003). "Bulletin 19 of the International Leonid Watch: Population index study of the 2002 Leonid meteors". *WGN*, **31:3**, 77–87.
- Arlt R. (2004). Private communication.
- Arlt R. and Gyssens M. (2000). "Bulletin 16 of the International Leonid Watch: Results of the 2000 Leonid meteor shower". *WGN*, **28:6**, 195–208.
- Bellot Rubio L. (1995). "Effects of a dependence of meteor brightness on the entry angle". *Astronomy and Astrophysics*, **301**, 602–608.
- Gural P. (2001). "Meteor observation simulation tool". In Triglav M., Knoëfel A., and Trayner C., editors, *Proc. IMC 2001, Cerklno, Slovenia, 2001 Sept 20–23*, pages 29–35. IMO, Potsdam, Germany.
- Gural P. (2003). "Best viewing direction for visual meteor observations". *Meteor Trails*, **18**, 3–7.
- Gural P. and Jenniskens P. (2000). "Leonid storm flux analysis from one Leonid MAC video AL50R". *Earth Moon and Planets*, **82–83**, 221–247.
- Hoffmeister C. (1948). *Meteorströme*. J.A. Barth, Leipzig.
- Koschack R. and Rendtel J. (1990a). "Determination of spatial number density and mass index from visual meteor observations (I)". *WGN*, **18:2**, 44–58.
- Koschack R. and Rendtel J. (1990b). "Determination of spatial number density and mass index from visual meteor observations (II)". *WGN*, **18:4**, 119–140.
- Kresakova M. (1966). "The magnitude distribution of meteors in meteor streams". *Contributions of the Astronomical Observatory Skalnaté Pleso*, **3**, 75–109.
- Prentice J. (1953). "The hourly rate of the Quadrantid meteor shower at maximum". *Journal of the British Astronomical Association*, **63**, 175–186.
- Rendtel J., Arlt R., and McBeath A. (1995). *Handbook for Visual Meteor Observers, IMO Monograph No. 2*. IMO, Potsdam.
- Roggemans P. (1989). *IMO Handbook for Visual Meteor Observations*. Sky Publishing Corp.
- Van de Veen P. (1984). "The method of Öpik — a call to do it differently". *Radiant (Journal of the DMS)*, **6**, 75–80.
- Van de Veen P. (1986a). "Observers and integrals — from cosine to probability function". *Radiant (Journal of the DMS)*, **8**, 1–5.

Van de Veen P. (1986b). "Simulating meteor observations — the computer as visual observer". *Radiant (Journal of the DMS)*, **8**, 41–45.

Zvolankova J. (1983). "Dependence of the observed rate of meteors on the zenith distance of the radiant". *Bulletin of the Astronomical Institute of Czechoslovakia*, **34**, 122–128.

## Appendix A

The Human Perception Model (HPM90) used in the simulation is a two-parameter function of the elongation angle  $R$  in degrees from the central point of vision and the meteor's magnitude distance  $\Delta m$  relative to the limiting magnitude. It is based on an empirical fit to the measurements published in (Koschack & Rendtel, 1990a,b). The expressions include a cutoff in elongation angle for each magnitude class as the functions used are only valid over a limited range. There are two functional expressions used to mimic the different perception responses above and below  $\Delta m = 3.89$  which are reasonably well matched at that boundary. Note that the expressions in A-1 (overpage) are given in terms of the base ten logarithm of the perception (i.e. Perception =  $10^{\log(p)}$ ).

This two parameter perception model can be reduced to a single function of the magnitude distance by averaging over all elongation angles out to  $52.5^\circ$ . This was done in a Monte Carlo fashion for high statistical significance using the baseline scenario and then fit to an eighth order polynomial. The base ten logarithm of the average perception  $\langle p \rangle$  for HPM90 is given by the expression in equation A-2 (overpage).

The equivalent fit for the Koschack and Rendtel (1990b, Table 15) data is given in equation A-3 (overpage).

The conversion of the mean magnitude distance from the limiting magnitude  $\langle \Delta m \rangle$  to the population index  $r$  for the HPM90 model is given by expression A-4. Note that the mean magnitude is assumed to be computed for magnitude bins of  $\Delta m = 0.5$  up to  $\Delta m = 14.5$  and no higher (e.g. for a  $\text{lm} = +6.5$  the magnitude bins contributing to the mean calculation are +6, +5 +4, +3, ..., -7, -8). This expression is valid for the mean magnitude range of  $\langle \Delta m \rangle = 2.0$  to 6.5 which corresponds to population indices between 5.0 and 1.4 respectively. The standard deviation in  $r$  given analytically in expression A-5 as a function of the number of meteors  $N$  used to form  $\langle \Delta m \rangle$ .

$$r = 0.9487 - 4.643x + 7.0417x^2$$

$$\text{where } x = \log_{10}(\log_{10} \langle \Delta m \rangle) \quad (\text{A-4})$$

$$\sigma_r = [0.0174 - 0.003368r + 0.01885r^2]/N^{1/2} \quad (\text{A-5})$$

Table 1 is based on expressions A-4 and A-5 of population index and its standard deviation versus mean magnitude,  $N = 100$  meteors, the HPM90 model, and the baseline shower parameters.

$$\begin{aligned}
&\text{if } \Delta m < -2 + R/10 & \log_{10} p(R, \Delta m) &= -6 \\
&\text{else if } \Delta m > 3.89 & \log_{10} p(R, \Delta m) &= 1 - \exp(3.7 \cdot 10^{-5} 2^{4-\Delta m} R^{2.5}) && \text{for } R \neq 0 \\
&& &= 0 && \text{for } R = 0 \\
&\text{else} & \log_{10} p(R, \Delta m) &= -1.8104 + 0.707d + 0.0168d^2 - 0.0103d^3 \\
&& & \quad -0.00689d^4 + 0.00111d^5 \\
&& \text{where } d &= \Delta m + 0.11 - 0.03R - 0.00057R^2
\end{aligned} \tag{A-1}$$

$$\begin{aligned}
&\text{if } \Delta m < 0.0 & \log_{10} \langle p \rangle (\Delta m) &= -6 \\
&\text{else if } \Delta m > +8.5 & \log_{10} \langle p \rangle (\Delta m) &= 0 \\
&\text{else} & \log_{10} \langle p \rangle (\Delta m) &= -2.7220 + 1.0317\Delta m - 0.30865\Delta m^2 + 0.20799\Delta m^3 \\
&& & \quad -0.0832\Delta m^4 + 0.016815\Delta m^5 - 0.0018129\Delta m^6 \\
&& & \quad +0.00010042\Delta m^7 - 2.2553e-06\Delta m^8
\end{aligned} \tag{A-2}$$

$$\begin{aligned}
&\text{if } \Delta m < -0.4 & \log_{10} \langle p \rangle (\Delta m) &= -6 \\
&\text{else if } \Delta m > +7.7 & \log_{10} \langle p \rangle (\Delta m) &= 0 \\
&\text{else} & \log_{10} \langle p \rangle (\Delta m) &= -2.6152 + 1.5254\Delta m - 0.73561\Delta m^2 + 0.19182\Delta m^3 \\
&& & \quad +0.023254\Delta m^4 - 0.024201\Delta m^5 + 0.0052161\Delta m^6 \\
&& & \quad -0.00048246\Delta m^7 + 1.678e-5\Delta m^8
\end{aligned} \tag{A-3}$$

Table 1 – Population index  $r$  and its standard deviation  $\sigma_r$  for a range of magnitudes  $\Delta m$ . Derived with equations A-4 and A-5 using  $N = 100$  meteors, the HPM90 model and the baseline shower parameters.

$\Delta m$	$r$	$\sigma_r$	$\Delta m$	$r$	$\sigma_r$	$\Delta m$	$r$	$\sigma_r$	$\Delta m$	$r$	$\sigma_r$
			4.630	2.0	0.0086	3.135	3.0	0.018	2.463	4.0	0.031
			4.402	2.1	0.0093	3.044	3.1	0.019	2.427	4.1	0.032
			4.203	2.2	0.0101	2.958	3.2	0.020	2.380	4.2	0.034
			4.021	2.3	0.0109	2.903	3.3	0.021	2.343	4.3	0.035
6.492	1.4	0.0049	3.856	2.4	0.0118	2.813	3.4	0.022	2.300	4.4	0.037
6.143	1.5	0.0055	3.704	2.5	0.0127	2.746	3.5	0.024	2.246	4.5	0.038
5.798	1.6	0.0060	3.571	2.6	0.0136	2.710	3.6	0.025	2.227	4.6	0.040
5.471	1.7	0.0066	3.446	2.7	0.0146	2.632	3.7	0.026	2.171	4.7	0.042
5.167	1.8	0.0072	3.334	2.8	0.0156	2.570	3.8	0.028	2.133	4.8	0.044
4.885	1.9	0.0079	3.219	2.9	0.0166	2.536	3.9	0.029	2.109	4.9	0.045

# A spreadsheet that calculates meteor orbits

Marco Langbroek<sup>1</sup>

The author has written an MS Excel spreadsheet application called METORB08.XLS which calculates a meteor's orbital elements from its apparent radiant position and initial speed. It can be downloaded from URL <http://home.wanadoo.nl/marco.langbroek> along with a suite of other meteor-related Excel applications.

Received 2004 August 1

## 1 Introduction

Amongst the available public domain software for meteor astronomy, software that calculates a meteor's orbit from radiant and speed data is hard to find. Frustrated by this, this author wrote a software application himself, that is available for download from his website. It is an application in Microsoft Excel, a widely used spreadsheet running under Windows.

## 2 The spreadsheet

The spreadsheet file, called METORB08.XLS, which is 95 kB in size, consists of three sheets. Sheet 1, called 'input', is where the basic data input has to be done. Sheet 2, 'output', gives the output. Sheet 3, 'references', details which equations from which publications were used. Consulted publications providing the necessary equations were: Lovell (1954); Whipple and Jachia (1957); Ceplecha (1987); Jenniskens and De Lignie (1987); and Meeus (1991).

The spreadsheet corrects the observed radiant location and the initial speed ( $V_\infty$ ) for diurnal aberration (the rotation of the Earth around its polar axis), and corrects the speed and radiant location for gravitational pull (including zenith attraction). Thus, the geocentric radiant and speed are obtained. These are transformed into ecliptic coordinates. After correction for the Earth's movement around the Sun, the heliocentric radiant and speed are obtained, and from these the orbital elements are computed.

## 3 Input data

The spreadsheet asks for input of the following data:

1. geographic coordinates of the meteor;
2. date and time of appearance of the meteor (in UTC);
3. azimuth and altitude of the apparent radiant, i.e. flight azimuth and entry angle of the meteor;
4. initial speed of the meteor ( $V_\infty$ );
5. the Earth's heliocentric ecliptic X, Y, Z position and orbital speed at the time of the meteor;
6. optional ID number of the meteor.

The necessary heliocentric ecliptic X, Y, Z coordinates and orbital speed of the Earth can be taken from the

Astronomical Almanac, or calculated using for example Planeph 4.2 software, which is DOS freeware by G. Francou & J. Chapront of the French Bureau des Longitudes, available at: <ftp://cdsarc.u-strasbg.fr/pub/cats/VI/87/>.

## 4 Output data

The spreadsheet returns the following output:

1. RA and Dec of the apparent radiant;
2. RA and Dec of the geocentric radiant, and the geocentric speed;
3. the heliocentric radiant  $\lambda$ ,  $\beta$  and the heliocentric speed;
4. orbital elements  $q$ ,  $a$ ,  $e$ ,  $i$ ,  $\omega$ ,  $\Omega$  and  $\pi$ ;
5. values for  $1/a$ , aphelion distance  $Q$ , and the solar longitude at the time of the meteor;
6. additional information on the orbit, including: orbital period of the meteoroid; number of days the meteoroid was from passing perihelion; in which node the Earth met the meteoroid; indication whether the orbit is prograde or retrograde; indication whether the orbit is elliptic or hyperbolic; indication whether the orbit is Jupiter-crossing; and the ratio of the meteoroid's orbital period to Jupiter's orbital period.

## 5 Accuracy

This is an amateur's attempt at writing orbital reduction software. This author does not pretend that the spreadsheet performs at the level of state-of-the-art professional software like the Czech FIRBAL software of the Ondřejov group (Ceplecha, 1987), and anyone using it should not expect such professional accuracy. Nevertheless, a test on several photographic multistation meteors obtained by the Dutch Meteor Society for which orbits have been calculated with the mentioned FIRBAL software (Betlem et al., 1998), shows that the spreadsheet performs well.

Three randomly picked test cases are provided in order to illustrate this: two of these concern very slow fireballs, for which the effects of zenith attraction and diurnal aberration are notable. The original orbits have been published by Betlem (1989a,b; 1993) and the numbers refer to the catalogue number in the DMS database (Betlem et al., 1998). The  $D'$  criterion of Drummond (1981) is given in each case as a measure of how well the two computed orbits compare. The results are given in Table 1.

<sup>1</sup>Diefsteeg 1, NL-2311 TS Leiden, the Netherlands.  
Email: [meteorites@dmsweb.org](mailto:meteorites@dmsweb.org)

Table 1 – Three tests of the spreadsheet, showing comparisons with results from the Ondřejov FIRBAL software.

Test Case 1: DMS 1988035 (1988 Nov 3,  $V_{\infty}$  16.2 km/s, RA  $299^{\circ}16$ , Dec  $+41^{\circ}05$ ).  $D' = 0.0069$

	$V_{\text{geo}}$	$RA_{\text{geo}}$	$DEC_{\text{geo}}$	$q$	$a$	$e$	$i$	$\omega$	$\Omega$
METORB08	11.8	293.69	+37.88	0.992	2.35	0.579	15.49	179.70	221.75
FIRBAL	11.9	293.67	+37.89	0.992	2.40	0.587	15.63	179.67	221.75

Test Case 2: DMS 1989001 (1989 Feb 7,  $V_{\infty}$  18.9 km/s, RA  $126^{\circ}84$ , Dec  $+63^{\circ}60$ ).  $D' = 0.0020$

	$V_{\text{geo}}$	$RA_{\text{geo}}$	$DEC_{\text{geo}}$	$q$	$a$	$e$	$i$	$\omega$	$\Omega$
METORB08	15.1	134.06	+64.02	0.899	2.21	0.594	16.97	220.32	319.15
FIRBAL	15.1	133.64	+64.12	0.900	2.23	0.596	16.94	220.04	319.15

Test Case 3: DMS 1993004 (1993 Mar 15,  $V_{\infty}$  26.9 km/s, RA  $290^{\circ}96$ , Dec  $+57^{\circ}22$ ).  $D' = 0.0049$

	$V_{\text{geo}}$	$RA_{\text{geo}}$	$DEC_{\text{geo}}$	$q$	$a$	$e$	$i$	$\omega$	$\Omega$
METORB08	24.4	294.48	+56.70	0.952	2.03	0.530	40.69	151.22	354.60
FIRBAL	24.3	294.41	+56.74	0.952	2.01	0.526	40.57	151.24	354.60

## 6 Use of the spreadsheet

The author has made the spreadsheet available for use on his website. It can be downloaded from URL: <http://home.wanadoo.nl/marco.langbroek>. When results obtained with the spreadsheet are used in presentations or publications, this WGN paper should be cited.

On the same URL, several other meteor-related Excel applications can be found. The application D\_CRIT.XLS for example compares two sets of orbital elements using the D' criterion of Drummond (1981). An earlier version of the Meteorb spreadsheet, called METORB07.XLS, calculates orbital elements from a geocentric radiant and speed. A spreadsheet GEO\_RAD.XLS converts an apparent radiant to a geocentric radiant (Meteorb08 is the integration of both these spreadsheets into one).

## Acknowledgments

Marc de Lignie, Casper ter Kuile and Carl Johannink all contributed in problem-solving during development of the spreadsheet, and/or helped gathering publications on orbital determination. I am much indebted to them.

## References

- Betlem H. (1989a). “De vuurbol van 7 februari 1989”. *Radiant*, **11**, 40–41.
- Betlem H. (1989b). “Rekenwerk aan simultaanopnamen”. *Radiant*, **11**, 42–46.
- Betlem H. (1993). “Vuurbollen. Maart-April-Mei 1993”. *Radiant*, **15**, 87–91.
- Betlem H., Ter Kuile C., De Lignie M., Van 't Leven J., Jobse K., Miskotte K., and Jenniskens P. (1998). “Precision meteor orbits obtained by the Dutch Meteor Society — Photographic Meteor Survey 1981–1993”. *Astron. Astroph. Supplement*, **128**, 179–185.
- Cepplecha Z. (1987). “Geometric, dynamic, orbital and photometric data on meteoroids from photographic fireball networks”. *Bull. Astron. Inst. Czech.*, **38**, 222–234.
- Drummond D. (1981). “A test of comet and meteor shower associations”. *Icarus*, **45**, 545–553.
- Jenniskens P. and De Lignie M. (1987). “Baanelementen: een meteorbaan om de zon”. *Radiant*, **9**, 10–17.
- Lovell A. (1954). *Meteor Astronomy*, chapter V. Clarendon press, Oxford.
- Meeus J. (1991). *Astronomical Algorithms*. Willman-Bell, Richmond, VA, USA.
- Whipple F. and Jacchia L. (1957). “Reduction methods for photographic meteor trails”. *Smiths. Contr. Astrophys.*, **1**, 183–206.

# SPA Meteor Section Results: January-March 2002

*Alastair McBeath*<sup>1</sup>

Highlights from data presented to the SPA Meteor Section from January to March 2002 are analyzed and discussed. Some notes on the revised schedule for these reports, and how the radio meteor material is to be tackled in future, are given too. A Quadrantid maximum almost exactly as predicted, around January 3, 17<sup>h</sup>56<sup>m</sup> UT ( $\lambda_{\odot}$  (eq. 2000.0) = 283°16'), was suggested by the available results, perhaps with an EZHR  $\sim 140 \pm 15$ . No secondary maximum, some 9<sup>h</sup>–12<sup>h</sup> after the main peak, was found in 2002. February and March were notable for a number of sporadic fireballs, the best-seen of which was on March 13/14, at 19<sup>h</sup>54<sup>m</sup>  $\pm$  2<sup>m</sup> UT. It probably flew high over part of the western Isles and the central-western Scottish mainland of the UK.

Received 2004 April 28

## 1 Introduction

Various problems over recent years for the author have forced a revision in how these report articles are presented. The format has now shifted from a bimonthly to a quarterly review of highlights from the data received. In addition, due to greatly increased quantities of radio data, it is no longer possible to continue the very detailed Forward Scatter Meteor Year analyses. Instead, regular attention will be concentrated on examining radio data during the following periods:

The Quadrantid maximum in January; the January 20–26 period; the Lyrid maximum in April; the  $\eta$ -Aquarid maximum in early May; the June daytime streams peaking in early to mid month; the June Boötids/ $\beta$ -Taurid epoch in late June to early July; the SDA and CAP maxima in late July; the Perseid maximum in mid-August; the September 15–17 period; the daytime Sextantid maximum in late September; the Draconid epoch of early October; the Orionid maximum (including the occasional October 17–18 peak) through to the potentially enhanced Taurid rates in late October; the Leonid and  $\alpha$ -Monocerotid maxima in mid-November; the Geminid and Ursid maximum epochs in December.

Dependent on the nature of the source and the duration of its stronger activity, each epoch will last some 5–10 days, to provide comparison data some way before and after the peak, or the suspected active period. Other times of interest, when unusual activity may have manifested, as identified by observers or following predictions in specific years, will be checked too.

The volume of radio data now being presented means it is necessary and desirable to include more stringent quality-control measures, to ensure the analysis of the raw data advocated in these reports over the last decade, continues to produce meaningful results. In this and future analyses, radio data recorded continuously, where periods of interference or other problems were clearly identified, will be given greatest weight. Other results will have increasingly less weight away from this ideal. However, it has become obvious in recent years that not all radio systems have successfully detected even the major showers. Consequently, all radio data will now be checked near the stronger major peaks of showers detectable from the observer's

location. Systems which show little or no enhancement during the shower's peak, or which reveal significantly anomalous diurnal activity beyond what is normally seen from the sporadics, will not be considered viable for further investigation after that, until the next major shower, when a fresh test will be made. Systems not operated continuously will be checked only after the other data, primarily for confirmation of any details already established, where that has been achieved, or to assist during times of serious interference.

Those datasets with obvious unidentified interference, where interference periods were not recorded, or where there was some other problem or doubt regarding the results, will not be used at all. While all observers will remain listed, and rightly thanked for the effort involved in even trying to make some radio observations, and ensuring they are made more widely available, the radio hours' totals given in this and subsequent reports will show only the amount of viable data.

## 2 The quarter's totals and observers

Table 1 gives the monthly tallies for the first quarter of 2002.

Lunar circumstances were very poor for the Quadrantid peak, with a waning gibbous Moon on January 3–4. Then the weather seems to have been a greater problem in the rest of the quarter, aside from the distraction of Comet Ikeya-Zhang (C/2002 C1) in March, that is.

The radio data came from Dirk Artoos (Belgium) and the following Radio Meteor Observation Bulletin (RMOB; website: [www.rmob.org](http://www.rmob.org)) observers, whose data was provided by editor Chris Steyaert, from RMOBs 102–104, 2002 January to March, inclusive:

Enric Fraile Algeciras (Spain), Mike Boschat (Nova Scotia, Canada), Jeff Brower (Colorado, USA), Maurice de Meyere (Belgium), Minoru Ehara (Japan), Ghent University (Belgium), Patrice Guirin (France), Toshihide Miyake (Japan), Stan Nelson (New Mexico, USA), Hiroshi Ogawa (Japan), Sadao Okamoto (Japan), Robert Savard (Quebec, Canada), Dave Swan (England), Pierre Terrier (France), Garfield Tsao (Taiwan, China), Ilkka Yrjölä (Finland).

The video results came from observers submitting data to the German Arbeitskreis Meteore (AKM; website: [www.meteoros.de](http://www.meteoros.de)), as reported in their journal *Meteoros* 5:2–5:4 (2002) inclusive, sent in by Ina Rendtel:

<sup>1</sup>12a Prior's Walk, Morpeth, Northumberland, NE61 2RF, England, UK. Email: [meteor@popastro.com](mailto:meteor@popastro.com)

*Table 1* – Visual, video and radio hours' totals, visual and video meteor numbers recorded (with a partial breakdown of visual types), per month.

Month	Visual	QUA	Meteors	Video	Video meteors	Radio
January	69 <sup>h</sup>	318	640	625 <sup>h3</sup>	3880	5010 <sup>h</sup>
February	53 <sup>h5</sup>	–	291	382 <sup>h5</sup>	2616	4209 <sup>h5</sup>
March	24 <sup>h6</sup>	–	97	469 <sup>h5</sup>	2787	5318 <sup>h</sup>

Orlando Benitez-Sanchez (Canary Isles), Steve Evans (England, who also provided preliminary notes on his Quadrantid observing directly), Detlef Koschny (Netherlands), Rob McNaught (New South Wales, Australia), Sirko Molau (Germany), Mirko Nitschke (Germany), Steve Quirk (Australia), Jürgen Rendtel (Germany), Ulrich Sperberg (Germany), Rosta Stork (Czech Republic), Jörg Strunk (Germany).

Visual observations were produced by:

American Meteor Society (AMS; website: [www.amsmeteors.org](http://www.amsmeteors.org)) reporters, extracted from summaries in the AMS' journal Meteor Trails 16 (September 2002), sent via editor and active observer Bob Lunsford (California, USA): Jure Atanackov (Slovenia), Edwin Jones (Arizona, USA), Tomislav Jurkic (Croatia), Javor Kac (Slovenia), Thomas Lazuka (Illinois, USA), Pierre Martin (Ontario, Canada), Paul Martsching (Iowa, USA), Bert Matous (Kansas, USA), Jim McGraw (Iowa, USA), Jure Zakrajsek (Slovenia); AKM members (all in Germany): Frank Enzlein, Christoph Gerber, Daniel Grün, Martin Hörenz, Ralf Kuschnik, Hartwig Lüthen, Sven Näther, Jürgen Rendtel, Roland Winkler; Terry Churms (England), Jonathan Shanklin (England).

### 3 January

The main interest during the month centred on the Quadrantid peak, due around 18<sup>h</sup> UT on January 3 (McBeath & Arlt, 2001, p. 2). Bright moonlight, and typically poor northern-hemisphere winter weather did little to assist visual watchers, although even the radio coverage was a little patchy. This latter was not helped as the maximum timing coincided with part of the Quadrantid radiant's lowest elevation during the day for European observers, as Figure 1 illustrates.

The impression from most European radio datasets was similar to that in Figure 1a), with two peaks on January 3–4, separated by something of a dip, in time to the lowest Quadrantid radiant elevation. This often indicates stronger activity was actually occurring throughout the interval, though not always. In North America (Figure 1b), two peaks of a different character were found, while in Japan, just a strong, single maximum occurred on January 3 (as shown in Figure 1c).

Close inspection of some European datasets indicated a minor peak during the radiant elevation's lowest time on January 3, which, in conjunction with the North American and Japanese data, suggested this was close to the real maximum. The few visual results from the same interval in Europe implied a maximum

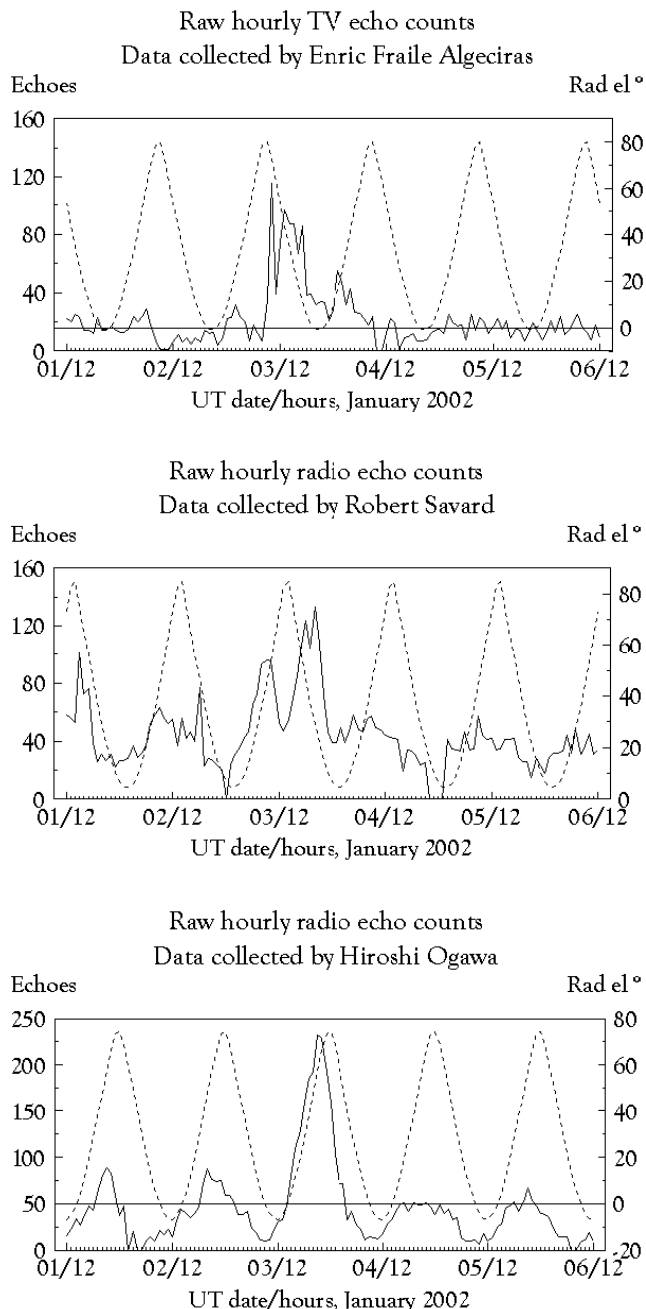


*Figure 1* – Sample raw hourly radio meteor echo count graphs, from data collected over the Quadrantid maximum by: a) Enric Fraile Algeciras (Europe); b) Robert Savard (North America); and c) Hiroshi Ogawa (Japan). Echo counts are shown by the irregular lines, keyed to the left-hand *y*-axes. Drops to zero in b) and c) (only) show times when interference prevented data-gathering. The thinner, daily-symmetric, curves, keyed to the right-hand *y*-axes, give the Quadrantid radiant elevation per site. Note Robert Savard's data are those from RMOB 103 (February 2002), not 102, which were given as January's results in error.

around January 3, 18<sup>h</sup>2 UT. A crude estimate of the mean time of the various outlying European radio graph peaks, and the one North American dataset, gave January 3, 17<sup>h</sup>75 UT. A similarly crude average time for the peak ZHRs recorded by Japanese visual observers (Ogawa, 2002), yielded January 3, 17<sup>h</sup>94 UT. Combining all three averages, suitably weighted based on the agreement between different individual datasets, gave a rough Quadrantid maximum mean time of January 3, 17<sup>h</sup>94 (17<sup>h</sup>56<sup>m</sup>) UT, equivalent to  $\lambda_{\odot} = 283^{\circ}16$ , identical to the anticipated peak time. This is a pleasing result, if not an ideally-measured one. The radio data does at least infer a rough near-consensus for a peak between 17<sup>h</sup> and 20<sup>h</sup> UT then at least.

Individual visual ZHRs showed a large scatter, because of the low radiant elevation for Europe (and the bright Moon over Japan in the results previously published). A best-estimate, using  $r = 2.1$ , implies that a peak value of  $\sim 140 \pm 15$ , gives a useful ballpark figure, if one which may be somewhat inflated due to conditions.

There was no evidence in the post-maximum phase for any visual-radio signature of the possible second, weaker, maximum in the Quadrantids, some 9<sup>h</sup>–12<sup>h</sup> after the chief peak, in 2002. This secondary maximum was suggested by results from 2000, 2001 and 2003 (McBeath, 2000, 2001b, 2003).

The January 20–26 interval, perhaps producing rates from the minor January Coma Berenicids (cf. (McBeath, 2001b)), had a bright waxing Moon to contend with, and few visual watches were received as a result. In the European radio data, a minor peak was apparent around January 23 ( $\lambda_{\odot} = 303^{\circ}$ – $304^{\circ}$ ), which has been found for some years (McBeath, 2001a). The paucity of visual data is unhelpful in confirming if this may have been due to any potential January Coma Berenicid activity, unfortunately.

## 4 February and March

Both months provided the typically low activity expected of them for northern-hemisphere visual and radio observers. The main items of interest were a number of fireball sightings, as has been the case during both months in several years recently.

February 3/4 and 4/5 brought two bright fireballs for British witnesses, at the oddly coincidental time of  $\sim 06^{\text{h}}50^{\text{m}}$  UT on both dates. That on February 4/5 was seen from three sites in northern England and southern Scotland, but none of the observers was able to give a detailed enough account to allow a rough trajectory to be estimated.

Three more fireball sightings were received from central and northern England on February 8/9, about 01<sup>h</sup>29<sup>m</sup> UT, on a magnitude  $-8/-10$  meteor. Two of the observers were able to provide useful positional details, which showed the fireball descending almost vertically in the northern sky from the English Midlands. Regrettably, these two viewers were too close together to reliably triangulate to the trail, but the direction and elevation in the sky suggested the fireball may have passed above north-west England, and probably over part of southern Scotland too.

Of March's fireballs, only one was seen by multiple witnesses, a magnitude  $-5/-6$  event on March 13/14, around 19<sup>h</sup>54<sup>m</sup>  $\pm$  2<sup>m</sup> UT, from locations across northern England. Rough positional data, collected by the four observers involved, indicated the meteor had probably passed overhead across the Inner Hebrides and surrounding seas, and the central-western Grampian Mountains on the Scottish mainland. With all sightings from the southern side of the fireball's track only, and all considerably distant from it, it cannot be more precisely defined than this. Interestingly, three of the four observers were out examining Comet Ikeya-Zhang when the fireball flew over, the comet by chance being in the same general area of the sky as the fireball for all the people involved. Typically, the author, otherwise ideally-situated to have seen this meteor, retired indoors from a session observing the comet around 19<sup>h</sup>45<sup>m</sup> UT.

## 5 Acknowledgements

Grateful, if rather belated, thanks are expressed again to all contributors to this report.

## References

- McBeath A. (2000). "SPA Meteor Section results: January–February 2000". *WGN*, **28:6**, 232–236.
- McBeath A. (2001a). "The forward scatter meteor year: 2001 update". *WGN*, **29:3**, 85–92.
- McBeath A. (2001b). "SPA Meteor Section results: January–February 2001". *WGN*, **29:6**, 224–228.
- McBeath A. (2003). "SPA Meteor Section results: Preliminary 2003 Quadrantid report". *WGN*, **31:2**, 64–68.
- McBeath A. and Arlt R. (2001). *2002 Meteor Shower Calendar*. IMO, Potsdam.
- Ogawa H. (2002). "Quadrantids 2002 in Japan — final announce — (visual observation)". IMO-News e-mailing list, 2002 January 11.

# Boötids

## 2004 June Boötids: video images and low-resolution spectra of 7P/Pons-Winnecke debris

Peter Jenniskens<sup>1</sup>

A predicted encounter with the 1819, 1825, 1830, and 1836 dust ejecta of comet 7P/Pons-Winnecke on 2004 June 23 was observed from California using a low-resolution slit-less spectrograph. Six slow June Boötids of magnitude +0.4 to +2.3 were recorded in the  $17 \times 13$  degree field of view between 07<sup>h</sup>30<sup>m</sup> and 12<sup>h</sup>00<sup>m</sup> UT, with a noticeable lack of fainter meteors. In addition, two spectra were obtained from meteors just outside the field of view that show strong sodium emission and a weak magnesium line, on top of a faint continuum that lacks air plasma emissions. This report issued shortly after the observations presents preliminary results.

Received 2004 July 4

### 1 Introduction

Sergey Shanov and Sergey Dubrovsky (2004) pointed out that, on 2004 June 23, the Earth was to meet a cluster of dust trails from comet 7P/Pons-Winnecke ejected in 1819, 1825, and 1830 with a predicted peak time at 09<sup>h</sup>30<sup>m</sup> – 13<sup>h</sup>00<sup>m</sup> UT. Various distorted sections of the dust trails could lead to other encounters at 14<sup>h</sup>00<sup>m</sup>, 15<sup>h</sup>30<sup>m</sup> and 18<sup>h</sup>00<sup>m</sup> UT. Mikiya Sato (Sato, 2004) put the predicted peak between 12<sup>h</sup>30<sup>m</sup> (1830, 1825) and 19<sup>h</sup>30<sup>m</sup> UT (1813), depending on the dust trail approaching the Earth. Jeremie Vaubaillon (Vaubaillon, 2004), using massive-parallel supercomputing techniques, found a broad distribution of dust with a peak time centered on 11<sup>h</sup>00<sup>m</sup> UT. Rates were expected to be less than the outburst of 1998.

Visual observers reported an outburst of June Boötids from about June 22, 20<sup>h</sup> UT, until June 23, 23<sup>h</sup> UT (ZHR > 3), peaking at a rate of ZHR =  $18 \pm 2$  at June 23, 10<sup>h</sup>  $\pm$  1<sup>h</sup> UT, with a full-width-at-half-maximum of  $12 \pm 2$  hours (Shanov & Dubrovsky, 2004). The outburst was barely detected by forward meteor scatter stations of Global-MS-Net, suggesting that the shower was not rich in faint meteors. Figure 1 shows the counts by Esko Lyytinen in Finland. Indeed, the magnitude distribution index for the June Boötids was found to be only  $r = 2.3 \pm 0.2$ , with  $r_S = 3.2 \pm 0.3$  for the sporadic meteors observed in the same period by the same observers.

### 2 Video observations from California

The outburst occurred at the time of the SOFIA Upper Deck Science Opportunities workshop (June 22–23), providing a nice illustration of the kind of research proposed for future observations from the upper deck of the B747 aircraft that will be the Stratospheric Observatory For Infrared and Sub-millimeter Astronomy (SOFIA).

On the night of June 23, I deployed from my backyard in Mountain View, California (Longitude 122°1 W, Latitude +37°4 N) a slit-less spectrograph called ‘BETSY’, which is an intensified video camera (an XX1332 Image Intensifier coupled to a Hi-8 Sony CCD-

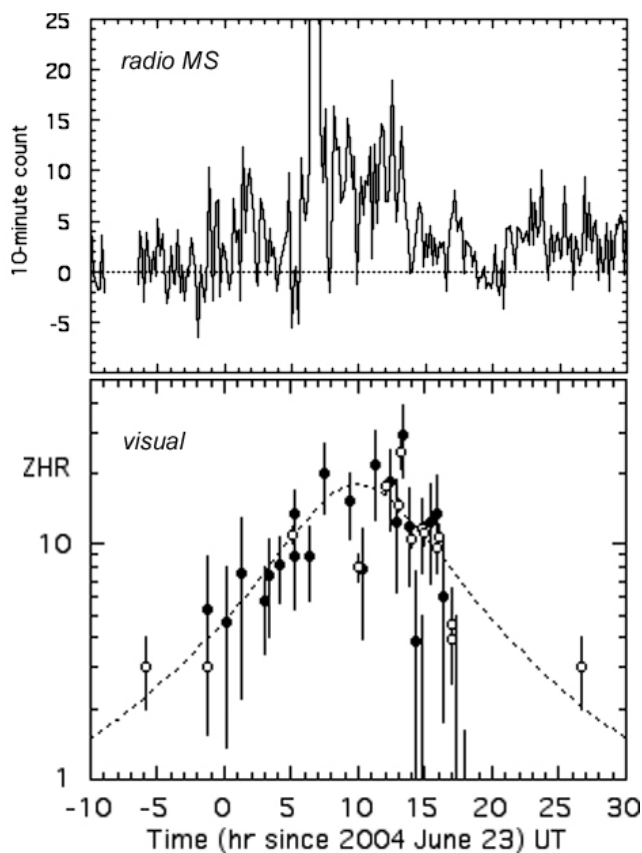


Figure 1 – Top: Raw 10-minute counts of radio reflections on a linear scale by Esko Lyytinen on 2004 June 23, after subtraction of the (scaled) rates from the same day in 2003. Gaps in the data are due to Aurora. Bottom: ZHR curve on logarithmic scale from visual observations by Robert Lunsford, Lew Gramer, Pierre Martin, Westley Stone, Roberto Haver, Mikiya Sato, Tomoko Sato, and Kazumi Terakubo. Also included are results summarized in the IMO and NMS Shower Circulars, with Japanese ZHR values scaled to match those from the USA (Arlt, 2004; Ogawa, 2004).

TRV69E PAL Handycam Vision camcorder) with a ‘De Oude Delft’  $f = 105$  mm  $f/0.75$  RAYXAR lens and a 230 lines/mm grating. The field of view is  $17 \times 13$  degrees. Because of city lights, the lens was stopped down to perhaps  $f/1.4$  and the star limiting magnitude of the camera was about +6.3.

<sup>1</sup>SETI Institute, 515 Whisman Road, Mountain View, CA 94043, USA. E-mail: pjenniskens@mail.arc.nasa.gov

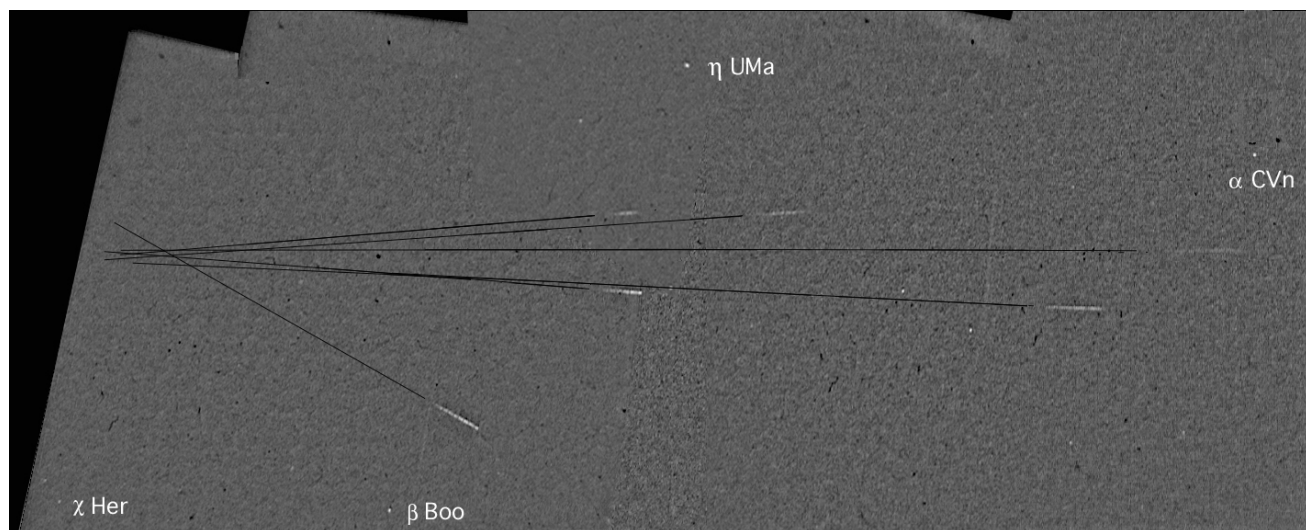


Figure 2 – A mosaic of video frames with June Boötids meteors. Each meteor image was compiled by pasting the track from four average frames, so that the meteors appear up to a factor of four less bright than the star background.

Observations were made from 07<sup>h</sup>30<sup>m</sup>30<sup>s</sup> to 08<sup>h</sup>38<sup>m</sup>25<sup>s</sup> UT, from 09<sup>h</sup>25<sup>m</sup>09<sup>s</sup> – 10<sup>h</sup>53<sup>m</sup>24<sup>s</sup> UT, and from 11<sup>h</sup>21<sup>m</sup>58<sup>s</sup> – 11<sup>h</sup>55<sup>m</sup>00<sup>s</sup> UT. Six characteristically slow June Boötids were detected at 07<sup>h</sup>36<sup>m</sup>36<sup>s</sup> (magnitude +1.8), 07<sup>h</sup>37<sup>m</sup>37<sup>s</sup> (+0.4, wake at end and faint spectrum), 08<sup>h</sup>14<sup>m</sup>11<sup>s</sup> (+2.3), 09<sup>h</sup>32<sup>m</sup>33<sup>s</sup> (+2.2), 10<sup>h</sup>19<sup>m</sup>23<sup>s</sup> (+1.4), and 10<sup>h</sup>45<sup>m</sup>05<sup>s</sup> (+2.2) UT. Magnitudes were derived by comparing the integrated intensity of the meteor images (400–880 nm) with those of nearby stars, and calibrated to the V-magnitude of those stars. In addition, sporadic meteors (all much speedier) were detected at 08<sup>h</sup>38<sup>m</sup>22<sup>s</sup> (+1.7), 09<sup>h</sup>41<sup>m</sup>21<sup>s</sup> (–0.9, consisting of two fragments trailing each other, spectrum), 09<sup>h</sup>57<sup>m</sup>10<sup>s</sup> (+3.3) and 10<sup>h</sup>29<sup>m</sup>50<sup>s</sup> (+3.0), all times UT.

Bob Lunsford noticed that many meteors appeared to peak at +2 magnitude (+2.20 on average). All my June Boötids, too, are between magnitude +0.4 and +2.3, with a noticeable lack of meteors in the range +3 and +4 magnitude, which should have been detected. This suggests that the distribution may not have been exponential towards fainter meteors. That would be consistent with the relative poor showing in meteor scatter observations.

My two first meteors occurred one minute apart. Bob Lunsford, who observed from Pine Valley in southern California, saw flurries of June Boötids at 09<sup>h</sup>13<sup>m</sup> (5), 09<sup>h</sup>37<sup>m</sup> (6), and 10<sup>h</sup>30<sup>m</sup> UT (5) from a location about 600 km further south from my site. However, I did not detect June Boötids during the time intervals reported by Bob, suggesting that any clustering of meteoroids occurred on a spatial scale of less than 600 km.

The June Boötids are compiled in Figure 2 by averaging sets of four frames and pasting those together into a single image, then matching the different video fields. A high-pass filter was used to remove the sky background. A sharp radiant is found at about  $\alpha = 232^\circ$ ,  $\delta = +49^\circ 5'$  (read from a star chart), mostly determined by the final June Boötid at 10<sup>h</sup>45<sup>m</sup>05<sup>s</sup> UT, when the radiant was at an elevation of 27°. With a theoretical geocentric entry speed of 14.1 km/s, the zenith attraction

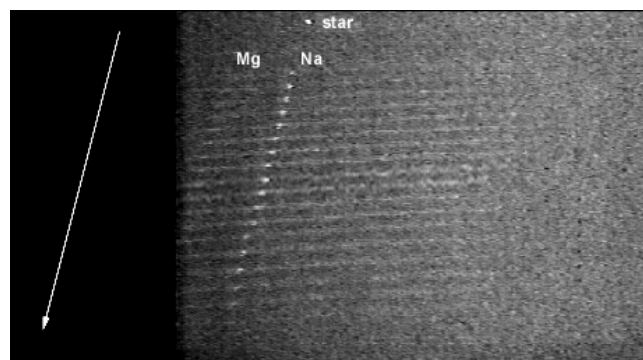


Figure 3 – The 400–880 nm spectrum (left to right) of the 2004 June 23, 10<sup>h</sup>23<sup>m</sup>02<sup>s</sup> UT June Boötid. Individual spectra are displaced for clarity. The meteor appeared just outside the field of view.

is  $3^\circ 3'$ , putting the true radiant at about  $\alpha = 227^\circ 3'$ ,  $\delta = +48^\circ 1'$  (J2000). This result will be improved after astrometric reduction, which is postponed until later.

Sato put the radiant of the 1830-1 dust trail at 223 $^\circ$ 0', +47.1 ( $v_g = 14.14$  km/s), that of 1825-1 at 223 $^\circ$ 0', +47.0 (14.13 km/s), and that of 1813-3 at 223 $^\circ$ 1', +47.0 (14.10 km/s), that of 1813-2 at 223 $^\circ$ 1', +46.9 (14.10 km/s). Hence, there is a significant discrepancy. The observed zenith attraction appears to be about two times larger than calculated.

### 3 Low resolution spectra

Two low-resolution spectra from June Boötids just outside the field of view were recorded at 07<sup>h</sup>50<sup>m</sup>07<sup>s</sup> and 10<sup>h</sup>23<sup>m</sup>03<sup>s</sup> UT, while a partial spectrum was measured for the +0.4 magnitude 07<sup>h</sup>37<sup>m</sup>37<sup>s</sup> UT meteor. From the relative intensity of the sodium line intensity, I deduce that the meteors just outside the field of view were magnitude –0.3 (07<sup>h</sup>50<sup>m</sup>07<sup>s</sup>) and –1.7 (10<sup>h</sup>23<sup>m</sup>03<sup>s</sup> UT), respectively. These magnitudes are in the range of those reported by visual observers.

The best spectrum is shown in Figure 3, and the extracted 1-dimensional spectrum (raw data, before correction for instrument sensitivity) is shown in Figure 4.

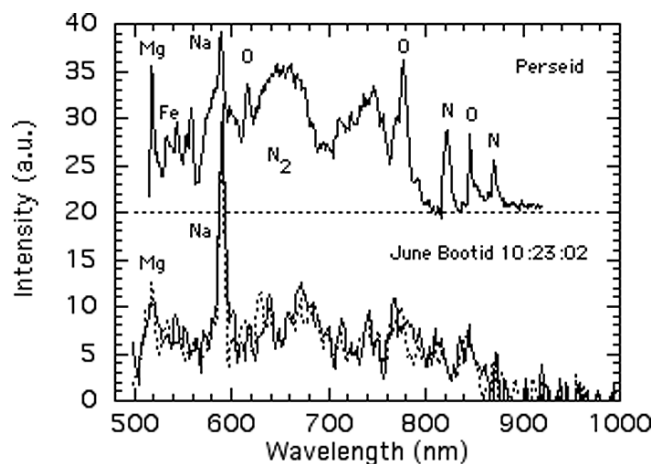


Figure 4 – Extracted spectrum for 2004 June 23, 10<sup>h</sup>23<sup>m</sup>02<sup>s</sup> UT June Boötids, without correction for instrument response curve. Dashed line: even fields, solid line: odd fields. A similar Perseid spectrum is shown for comparison, displaced upward by 20 units.

The June Boötids spectrum is dominated by strong sodium line emission, with only a weak magnesium line. The magnesium line has a later onset than the sodium line and the sodium line intensity after an early peak fades gradually when the meteor penetrates deeper into the atmosphere. This pattern is thought to be due to the more rapid loss of volatile minerals containing sodium and is only seen in meteoroids that fragment easily. Indeed, all June Boötids have a flat light curve, which is thought to result from high altitude fragmentation.

There is also a strong continuum visible that has a relatively small contribution from the First Positive system of the nitrogen molecule (which dominates Perseid spectra). There may be a very weak oxygen line at 777 nm in some parts of the spectrum. Metal atom line emissions of iron and calcium, as well as bands of metal oxides may dominate the continuum. This is work in progress.

## 4 Conclusion

A predicted outburst of June Boötids from comet 7P/Pons-Winnecke did occur and the forecast permitted spectroscopic and imaging observations that would not have been done otherwise. I find a compact radiant of meteoroids that are relatively fragile, as expected for an encounter with comet dust trails. Further analysis is needed to decide if the strong sodium emission is due to a lower excitation temperature in the emitting plasma, as suspected, or due to differences in the elemental composition of this grain of comet 7P/Pons-Winnecke.

## Acknowledgements

Global-MS-Net stations manned by Esko Lyytinen, Jeff Brower, and Ilka Yrjölä contributed meteor-scatter observations to this work. I thank NASA's Planetary Atmospheres program for support.

## References

- Arlt R. (2004). "June Boötids, visual data". In *IMO Shower Circular (June 25)*. IMO.
- Ogawa H. (2004). "Nippon Meteor Society announcement of June 24".
- Sato M. (2004). "June Bootids (from 7P Comet Pons-Winnecke) in 2004". <http://kaicho.pobox.ne.jp/tenshow/meteor/7p2004/e1.htm>.
- Shanov S. and Dubrovsky S. (2004). The original Russian website seems no longer to exist. However, several relevant postings by Shanov can be found on the meteorobs archive at <http://www.meteorobs.org/keysearch.html>.
- Vaubailon J. (2004). "2004 June Bootids forecastings". <http://www.imcce.fr/s2p/JB0/2004JB0.html>.

# History

## Meteor Beliefs Project: The Palladium in ancient and early Medieval sources

Alastair McBeath<sup>1</sup> Andrei Dorian Gheorghe<sup>2</sup>

An examination of the, apparently meteoritic, object, anciently called the Palladium after the Greek goddess Pallas Athene, is presented, as discussed in various ancient and early medieval sources. Although made of wood, the Palladium was believed to have fallen from the sky. In myths, it was a powerful totemic object, first at the legendary city of Troy, then later at Rome, and had magically protective properties associated with it. Despite its implausibly meteoritic nature, the Palladium can be suggested as supporting the case for ancient meteorite worship.

Received 2004 June 26

### 1 Introduction

The Palladium in ancient Greek mythology was an image of the goddess Pallas Athene. It was maintained in the citadel of Troy, and the city was believed safe from capture as long as the idol was there. Only after it was stolen did Troy fall to the besieging Achaian Greeks. It was taken eventually to Rome. The image was said to have fallen from heaven. Such is the information summarized in the more general dictionaries at least (e.g. (Simpson & Weiner, 1989, vol. XI, p. 99) or (Evans, 1970, pp. 796–797)).

This view is confirmed on the whole by Frazer's notes in his translation of Apollodorus' *Library* (Frazer, 1921, pp. 38–41, footnote 2). These provide a valuable synopsis of what was said of the Palladium in many ancient and medieval sources, through to the Tzetzes brothers in the 12th century AD. Frazer's evaluation of the beliefs about it included that the various sources to mention it often did not agree on the details, but that the majority favoured it being a small wooden image that had fallen from heaven, and that Troy remained safe from conquest as long as it was in the city.

In Greek, the word transliterates as 'palladion', which also occurs sometimes in English, but we have preferred the more usual spelling 'palladium' here. The idea that the image had fallen from the sky implies a possibly meteoritic origin for the tale. The importance of, and powers believed attached to, the Palladium are discussed in this article. Even if the original object was not a meteorite, such beliefs are still relevant to meteor and meteorite studies, in terms of popular understanding of objects which might fall from the heavens, and the consequent uses they might be put to, or the reverence that might be shown to them.

### 2 Dating the Palladium

Myths about the Trojan War which feature the Palladium are at first sight all relatively late. The earliest ancient authors who mention the Palladium directly,

and whose texts survive, date to the last century BC and the first two centuries AD, including Virgil (70–19 BC), Ovid (43 BC–17 AD), and Apollodorus' *Library* (probably written in the 1st or 2nd centuries AD judging by its word-usage, and certainly no earlier than the mid-1st century BC, from internal evidence). However, there are a few preserved summaries and fragments from much earlier. The first of these to include the Palladium seems to be the *Little Iliad* of Lesches (circa late 7th century BC), which survives only as an incomplete series of fragments scattered through other works (West, 2003, pp 118–143). The summary of the *Little Iliad* by Proclus in his *Chrestomathia*, ii, indicated it included the theft of the Palladium from Troy by Odysseus, with Diomedes' help. Other works, such as the play *The Laconian Women* by Sophocles (circa 497–406 BC), which survives as just two tiny fragments<sup>1</sup>, obviously dealt with the Palladium-theft episode too, from a comparison of the fragments with other versions of the legend, but the remaining texts fail to mention the Palladium directly.

Pherecydes, living in Athens in the early 5th century BC, wrote a lengthy text on Greek myths and legends which has regrettably been lost, again except for a few fragments which survive in other works. In one of these, summarized by Frazer (1921, p. 41, the continuation of footnote 2 from p. 38), he discussed palladia in general, indicating that there was believed to be more than one. Pherecydes derived the term from the Greek 'pallein' which he took to be the same as 'ballein', the verb 'to throw', because the objects were cast down from heaven. He said the palladia were forms not made by human hands. Modernly, we might call some of these simulacra, natural objects (such as rocks or plant roots) which appear to have a humanoid shape. The belief in multiple palladia can be found again much later, in Dionysius of Halicarnassus' *Roman Antiquities*, Book I.68–69 (Cary, 1937, pp. 223–229), for example. This was completed circa 7 BC. Dionysius suggested

<sup>1</sup>12a Prior's Walk, Morpeth, Northumberland, NE61 2RF, England, UK. Email: meteor@popastro.com

<sup>2</sup>Bd. Tineretului 53, bl. 65, ap. 40, sect. 4, București, Romania. Email: sarm@romwest.ro

<sup>1</sup>The two fragments of *The Laconian Women* are available in Greek, and English, translation as numbers 367 and 368 in *Sophocles: Fragments*, H. Lloyd-Jones (editor and translator), 1996, Harvard University Press (Loeb Classical Library imprint), pp. 196–197.

the name was applied to ‘the gifts of Athene’, without saying what these were, other than to note them as different to the statues of the Trojan gods.

Using ancient Greek art, particularly the Athenian black and red figure vases, which are very numerous artifacts, and can be quite well dated, illustrations of the Palladium seem to appear first in the early 5th century BC, although only on the red figure vases. The image shown is commonly of a female humanoid figure dressed in a thigh-length robe, with a crested Corinthian helmet pushed back on the figure’s head, holding a spear in its right hand and a large round shield in its left. It is about half the height of a man, where this can be judged. The spear, shield and pushed-back helmet are characteristics of Athene, who is almost always shown wearing or holding such items in Greek art. Consequently, she is one of the most easily recognised figures. For examples of the Palladium, see Fig. 363 in (Boardman, 1989, p. 188, and notes on p. 229) and Fig. 185 in (Boardman, 1975, p. 122, and notes on p. 232). The first image is much the clearer.

The most detailed, early, mythological treatment of the siege of Troy is of course Homer’s *Iliad*, probably written in the 8th century BC (as we discussed briefly in (McBeath & Gheorghe, 2003)). Homer made no mention of the Palladium at all, although the *Iliad* ended before the fall of Troy. There are references in Homer which are relevant to the matter of the Palladium however, which we shall discuss below. This all implies the Palladium may have entered the mythological canon sometime between the 8th and 7th centuries BC, and was increasingly common by the 5th century. It may have appeared as a mythological archetype to help explain the origins of palladia as a whole, or it may have been this originator itself, the later plurality due to copying, though neither view can be confirmed from the surviving sources.

### 3 Apollodorus’ *Library*

The best description of the Palladium, which included details of the image’s creation, and its arrival at Troy (also called Ilium), is in the *Library* attributed to Apollodorus. Apollodorus is otherwise unknown and, as we noted in Section 2, of uncertain dates. Despite these difficulties, the *Library* provides a clear, unaltered collection of Greek myths and legends as recorded in earlier sources, often giving more than one variant of a tale, with little attempt to reconcile the differences. Versions of myths given in the *Library* can be compared with those in older surviving texts, which show the accuracy of reproduction is exact enough, that other material which survives only in Apollodorus’ work can be regarded as equally reliable. Thus it is an excellent, indeed essential, work for students of ancient Greek mythology.

The *Library* Book III, XII.3 deals with the Palladium in detail (here taken from (Frazer, 1921, pp. 36–43)). Ilus was the son of Tros, eponymous king of the land of Troy (roughly equivalent to the coastal regions of modern Cannakale in north-western Asian Turkey).

He was given a dappled cow by the king of Phrygia (the lands immediately east of Troy, stretching into the western Anatolian mountains of modern Turkey) in accordance with an oracle, and was told to follow the cow until it lay down to rest. Where it did, there he should found his city. The cow lay down on the hill of Phrygian Ate, and there Ilus built his city Ilium. (Ate was Zeus’ eldest daughter, the goddess who blinded all men, and brought folly to mankind.)

Ilus then asked for guidance of the gods: *And having prayed to Zeus that a sign might be shown to him, he beheld by day the Palladium, fallen from heaven, lying before his tent. It was three cubits in height, its feet joined together; in its right hand it held a spear aloft, and in the other hand a distaff and spindle.* (Frazer, 1921, p. 39).

A cubit is the length of a human forearm and hand, approximately 45cm. This description is clearly not based on those in earlier Greek art, as the red figure vase description above demonstrates. The Palladium in Apollodorus is larger, and does not hold a shield, but a distaff and spindle. Thus the Apollodoran image is closer to representing the dichotomy of Athene’s masculine (warlike) and feminine (agricultural and virginal) qualities.

A little further on, the creation of the Palladium is described (op cit, pp. 40–43), which can be summarized as follows. After the goddess Athene’s birth from her father Zeus’ head, she was brought up by Triton, eponymous god of the river she was born beside (see *Library* Book I, III.6). The river was probably in Libya, or possibly was a stream in Boeotia on the Greek mainland. Triton had a daughter Pallas (literally meaning ‘maiden’ or ‘youth’). Both girls practised armed combat, but one day had a violent disagreement. Pallas was about to strike Athene when Zeus interposed the aegis, startling Pallas, who was fatally wounded by Athene. The aegis was a tasselled goatskin apron or shield, that bore the face of the Gorgon Medusa, which was later often an adjunct of the adult Athene’s.

Athene was appalled at her actions. Grief-stricken, she made a wooden image of Pallas, and wrapped the aegis about its breast. She set it up beside one of Zeus in the Olympian heaven, and paid it homage. Later, Electra, ancestress of Ilus, tried to hide from Zeus at the Palladium, but Zeus flung both the Palladium and Ate down into the Ilian country, caught and raped Electra. Electra was the Pleiad who disappeared (the mythological explanation for why only six naked-eye stars can be seen in the Pleiades star cluster, Messier 45, rather than the supposedly original seven). She was said to have done so because of the death of her and Zeus’ son Dardanus, and the loss of Troy — see Hyginus’ *Fabulae* CXCI ‘Hyas’ (Grant, 1960, pp. 148–149).

After he recovered it, Ilus built a temple for the Palladium, and honoured it. Although not stated by Apollodorus, Athene also took Pallas’s name and added it to her own, although there are other tales of why Athene was so-named (e.g. *Library*, Book I, VI.2).

As usual, Apollodorus made no comment concerning the obvious contradictions, such as having the Pal-

ladium land on the Hill of Ate, just as Ate was being flung from heaven too. These two falls from heaven carry us back to Homer.

#### 4 Homer's *Iliad*

As mentioned earlier, the Palladium does not appear in Homer's works, but both Ate and Athene descending meteorically to Earth do. These descriptions may be forerunners of the later Palladium beliefs.

Ate's powers of bringing folly and blinding people to the truth were once turned on her father Zeus. When he realized what had happened, he went wild, 'and immediately he seized Ate by her bright-tressed head, angered in his mind, and swore a mighty oath that never again to Olympus and the starry heaven should Ate come, who blinds all. So said he, and whirling her in his hand flung her from the starry heaven, and quickly she came to the tilled fields of men.' *Iliad* Book 19: 126–131 (Murray & Wyatt, 1999b, pp. 342–343).

This description of Ate's fall is an aside to the action at Troy, but from the discussion above regarding Apollodorus, there is a clear link between Ate and Troy. There is no mention here of Electra (Zeus is blinded over an entirely different matter in any case) or the Palladium, but the description calls to mind Greek imagery concerning comets and meteors, both of which are described as hairy in various places. 'Comet' in Greek is literally 'long-haired', while shaggy-haired 'goats' — Greek 'aiges', remembering Athene's goatskin aegis — were names for very bright meteors (cf. Aristotle's *Meteorologica* Book I, IV.1–35 (341 b 1), e.g. (Lee, 1952, pp. 28–33)).

The Athene passage occurs significantly earlier in the *Iliad*, in Book 4: 73–84. The deities on Olympus were discussing the war at Troy. Zeus ordered Athene to go there and make the Trojans break their oaths: 'So saying, he stirred on Athene, who was already eager, and down from the peaks of Olympus she darted. Just as the son of crooked-counselling Cronos sends a star to be a portent for seamen or for a wide army of warriors, a gleaming star, and from it the sparks fly thick; so darted Pallas Athene to earth, and down she leapt into their midst; and amazement came on all who saw her, on horse-taming Trojans and well-greaved Achaeans; and a man would turn to his neighbor and say: "We shall certainly again have evil war and dread din of battle, or else friendship has been placed between both armies by Zeus, who is for men the dispenser of battle."' (Murray & Wyatt, 1999a, pp. 168–171.) After her meteoric descent, Athene regained human form, but as a man, and went about her work.

The 'son of crooked-counselling Cronos' is of course Zeus. Although Athene clearly descended as a shooting-star long after Troy was founded, the fact that she, and only she, appears in such a specifically meteoric form in the *Iliad* seems quite plausibly the origin of, or at least a variant of, beliefs in the Palladium descending from the sky.

Spurred on by deities on both sides, the *Iliad* progresses from this point into a description of bloody and

violent warfare, which continues into Book 5, before the deities withdraw from the conflict for a time. The meteoric imagery here is thus used in a very negative sense, and could be interpreted as a dire warning.

#### 5 The Palladium's perceived importance

Ovid's *Fasti* VI: 417–436 (Frazer, 1931, pp. 350–353) provides a description of how the powers of the Palladium were discovered. The *Fasti* was almost complete by 8 AD, when Ovid's exile began (as we discussed previously (Gheorghe & McBeath, 2003)), and was further refined during it. In the *Fasti*, the image was described as being of Minerva, the Roman equivalent of Athene, which had leaped down from the sky to the hills of Troy. The god Mouse Apollo, Apollo Smintheus, was consulted in his sacred grove and answered: 'Preserve the heavenly goddess, so shall ye preserve the city. She will transfer with herself the seat of empire.' (*Fasti* VI: 427–428). Ovid continued that Ilus had kept the Palladium shut up on top of the citadel at Troy. Its care passed to his heirs in time, until the reign of Priam, Troy's king in the *Iliad*, when it was taken away by either Diomedes, Ulixes (anglicized to Ulysses in translation; in Greek Odysseus), both Achaian Greeks, or the Trojan Aeneas.

Indeed, there is little agreement among the sources to mention the Palladium's theft as to who actually stole it. The Greek versions had Diomedes and Odysseus going together to accomplish the task, but varied as to which one carried out the deed. Apollodorus provided a useful description of why and how the theft took place in his *Epitome* Book V: 10–13 (Frazer, 1921, pp. 222–229, including footnotes), with Odysseus as the actual thief. Frazer's footnote 2 to this section of the *Epitome* covers the alternative variants. These included that the Trojan Priestess of Athene, Theano, was said by some to have given the Palladium treacherously to the Greeks. This act, under threat of violence, sweetened by bribery, allowed Antenor to take the Palladium, according to Dictys of Crete's *Trojan War*, 5.8 (Frazer, 1966, p. 109), probably composed in the 1st century AD.

The Roman versions (as outlined in (Frazer, 1921, pp. 38–39, footnote 2)) had the Palladium remain in Troy until the city had fallen, after which Aeneas rescued it, and took it with him to Italy, depositing it in the Temple of Vesta at Rome. This is entirely incompatible with the Greek beliefs about Troy's security until the Palladium was removed, and ingenious reasons were thought up by the Romans to account for the discrepancy. These included that the Palladium displayed at Troy was really an exact copy, and that the true Palladium remained hidden until Aeneas carried it out of the city, and brought it eventually to Rome (according to Dionysius of Halicarnassus<sup>2</sup>). The idea that the Palladium's powers included controlling where the empire

<sup>2</sup>In *Antiquities of Rome*, Book I.69 and Book II.66 (Cary, 1937, pp. 226–229 and 502–507).

had its capital in Ovid's conception, fits to this Roman view of why it was taken to Rome. Ovid (*Fasti* VI: 437–454; (Frazer, 1931, pp. 352–353)) went on to describe in humorous terms the alarm shown in the Senate when Vesta's temple caught fire in 241 BC, almost burning the Palladium. What a potential end for a supposedly once-fiery meteoric object!

Virgil's *Aeneid* (Book II, 162–194) contains an interesting version of the Palladium's theft by Ulysses/Odysseus and Diomedes, which included the following description of portents generated by the idol after the event (lines 172–175):

*Scarcely was the image placed within the camp, when from the upraised eyes there blazed forth flickering flames, salt sweat coursed over the limbs, and thrice, wonderful to relate, the goddess herself flashed forth from the ground with shield and quivering spear.* (Fairclough, 1932, pp. 306–307).

Fairclough added a footnote to say that the unexpected triple appearance of Athene was described using phrasing indicating an apparition which showed itself suddenly, like lightning, a fascinating comment bearing in mind the link between meteors and lightning. In Virgil's tale, the seer Calchas interpreted these omens as meaning the Greeks needed to flee back to Argos on the Greek mainland, to seek fresh signs and portents.

Certainly, one of the alternative legends had the Palladium taken to Argos, and perhaps later to Sparta, although Pausanias (circa 120–180 AD) in his *Description of Greece* (Book II, XXIII.5) expressly denied this, saying Aeneas had taken it to Italy instead. Indeed, there is no real consensus between the ancient authors as to who of Odysseus, Diomedes or Aeneas took the Palladium away after its theft, or where it ended up. It does seem to have been considered important wherever it was taken though. Pausanias again (*Description of Greece* Book I, XXVIII.8–9 (Jones, 1918, pp. 150–151)) described the court of involuntary homicide at Athens, known as 'At Palladium'. In this, Diomedes landed by night in what he believed was hostile territory, but which was actually Phalerum in Attica, the Greek peninsula Athens is situated on. Troops led by Demophon, unaware of who had landed, attacked Diomedes' party, killing a number of them and capturing the Palladium. Demophon was the first to be tried at Athens 'At Palladium' as a result.

The Roman accounts do agree that the Palladium was at last brought to Rome, where it was still maintained in the temple of Vesta in Ovid's day and after. There is no news of what happened to it later, but it may have been lost in the sack of Rome by the Goths under Alaric in 410 AD. Procopius, writing in the mid-6th century AD (*History of the Wars* V.xv.8–14 (Dewing, 1919, pp. 150–153)), described how Diomedes fell ill, and was told he should only recover after he gave the stolen Palladium to a man of Troy. Consequently, he gave it to Aeneas after a chance meeting, and so it passed to the Romans. Procopius continued that the Romans in his day did not know where the statue was, but they had a copy chiselled in stone in the Temple of Fortuna, before a bronze statue of Athene, set up

under the open sky in the eastern part of the Temple. Procopius had clearly seen this copy for himself. He described it as showing a woman warrior, spear extended as if in combat, wearing a long chiton reaching her feet, the face seeming unlike the Greek portrayals of Athene, but more Egyptian in character. However, the Byzantines said the Emperor Constantine had dug up the statue in the Forum named after him, and set it in the Temple instead, again according to Procopius.

## 6 Some alternative tales

Dictys of Crete in his *Trojan War*, 5.5 (Frazer, 1966, p. 107), had the image of the Palladium fall from heaven, but while Ilus was building Minerva's (Athene's) temple for his new city. The structure was nearly finished when this occurred, but it had no roof, so the image was able to drop straight into its correct location within the temple.

Frazer's notes (1921, pp. 40–41) referring to Clement of Alexandria's *Protreptikos*, iv.47, mentioned Clement suggested the Palladium was made of the bones of Pelops. This may be due to a misreading of a source-text however, as Apollodorus' *Epitome* V.10 (ibid., pp. 224–225) cited three preconditions for the fall of Troy, the first of which was that the bones of Pelops must be brought to the besieging army. The second was that Neoptolemus must fight for the Achaeans, and the third was that the Palladium must be stolen. Clement's dates are circa 150–215 AD.

John Malalas in his *Chronicle*, Book 5.43, completed in the 560s AD, had a curious variant on the matter of the Palladium's first appearance. He described the image of Pallas as being small and wooden, enchanted to bring victory and to protect the city it was kept in safe from capture. So far, nothing unusual, but next follows a distinct break with past traditions:

*A certain Asios, a philosopher and wonder-worker, gave this Palladion to the emperor Tros when he was about to build the city. In gratitude and in his memory the emperor Tros gave the name Asia to all the land subject to him, which previously was known as Epitropos* (Jeffreys et al., 1986, p. 57).

Malalas is notable for a large number of variant retellings of ancient tales, although he was generally recounting these from other sources he used. While he drew on Dictys' *Trojan War* for much of his own version of the siege of Troy, this origin for the Palladium is not in Dictys' tale, and Malalas' version of the Palladium's arrival is certainly notable for being entirely non-meteoric!

## 7 Conclusion

Despite being a wooden idol, the Palladium clearly had meteoritic overtones, and was undoubtedly an object of veneration. Thus even if it were not a meteorite in any sense we would recognise now, it was formerly believed to have fallen from the skies, so can be taken as an example of ancient meteorite worship. The whole purpose of the Meteor Beliefs Project is to examine what people thought, and still think, to be true of meteors and allied

objects, without being scientifically correct in modern terms, after all. That other objects said to have fallen from the skies in ancient Greek and Roman traditions were also venerated is undoubted, and this is a topic we hope to return to later, as it is far too involved to be properly discussed now. Whether any of these objects were genuine meteorites is unknown, as none have survived to allow an examination today.

If anyone already has notes on the topic of ancient Greek and Roman meteorite worship they would like to discuss with us, we would welcome learning about them. As always, the Project moves forward faster and better with input from people besides ourselves. Also as usual, we would encourage anyone interested to read more fully in the texts we have merely skimmed or mentioned here. For those wanting to find out more about events surrounding the Palladium, the references given by Frazer (1921, pp. 38–41) are reasonably comprehensive for the surviving ancient and early medieval texts and fragments. Since the above article was submitted, a new reference for Lesches' *Little Iliad* has come to the authors' attention, of interest as it contains both the original Greek, and an English translation. It is in pages 118–143 of (West, 2003).

## 8 Afterword

Despite their similar names, the rare metallic element palladium, the asteroid 2 Pallas and the pallasite meteorites have no connection with either Pallas Athene or the ancient Greek Palladium. All three instead derive their names from the 18th century German natural historian, P.S. Pallas. He was the first to describe in detail a pallasite meteorite (in 1776), and after whom both the asteroid (discovered by Olbers in 1802) and the element (discovered by Wollaston in 1803) were later named.

## References

- Boardman J. (1975). *Athenian Red Figure Vases, The Archaic Period: A Handbook*. Thames & Hudson.
- Boardman J. (1989). *Athenian Red Figure Vases, The Classical Period: A Handbook*. Thames & Hudson.
- Cary E. (1937). *The Roman Antiquities of Dionysius of Halicarnassus, Volume I*. William Heinemann & Harvard University Press (Loeb Classical Library imprint).
- Dewing H. (1919). *Procopius, Volume III*. William Heinemann & G. P. Putnam's Sons (Loeb Classical Library imprint).
- Evans I. H. (1970). *The Wordsworth Dictionary of Phrase and Fable, Based on the Original Book of Ebenezer Cobham Brewer*. Wordsworth Reference, (1993 reprint).
- Fairclough H. R. (1932). *Virgil I: Eclogues, Georgics, Aeneid I–VI (Revised edition)*. William Heinemann Ltd & Harvard University Press (Loeb Classical Library imprint) (1967 reprint).
- Frazer J. G. (1921). *Apollodorus, The Library, Volume II*. Harvard University Press (Loeb Classical Library imprint), (1996 reprint).
- Frazer J. G. (1931). *Ovid, Volume V, Fasti*. Harvard University Press & William Heinemann Ltd. (Loeb Classical Library imprint) (1976 reprint).
- Frazer, Jr. R. M. (1966). *The Trojan War; The Chronicles of Dictys of Crete and Dares the Phrygian*. Indiana University Press.
- Gheorghe A. D. and McBeath A. (2003). "Meteor Beliefs Project: Meteoric references in Ovid's *Metamorphoses*". *WGN*, **31:5**, 145–147.
- Grant M. (1960). *The Myths of Hyginus*. University of Kansas Publications.
- Jeffreys E., Jeffreys M., Scott R., Croke B., Ferber J., Frankin S., James A., Kelly D., Moffatt A., and Nixon A. (1986). *The Chronicle of John Malalas*. Australian Association for Byzantine Studies, Byzantina Australiensia 4.
- Jones W. H. S. (1918). *Pausanias: Description of Greece, Volume I: Books I and II*. Harvard University Press & William Heinemann Ltd (Loeb Classical Library imprint) (1978 reprint).
- Lee H. D. P. (1952). *Aristotle, VII, Meteorologica*. Harvard University Press & William Heinemann Ltd. (Loeb Classical Library imprint).
- McBeath A. and Gheorghe A. D. (2003). "Meteor Beliefs Project: Three meteoric similes in *The Argonautica* of Apollonius of Rhodes". *WGN*, **31:3**, 99–100.
- Murray A. T. and Wyatt W. F. (1999a). *Homer, Iliad, Books 1–12 (2nd edition)*. Harvard University Press (Loeb Classical Library imprint).
- Murray A. T. and Wyatt W. F. (1999b). *Homer, Iliad, Books 13–24 (2nd edition)*. Harvard University Press (Loeb Classical Library imprint).
- Simpson J. A. and Weiner E. S. C. (1989). *Oxford English Dictionary (2nd Edition; 20 volumes)*. Oxford University Press.
- West M. (2003). *Greek Epic Fragments from the Seventh to the Fifth Centuries BC*. Harvard University Press (Loeb Classical Library imprint).

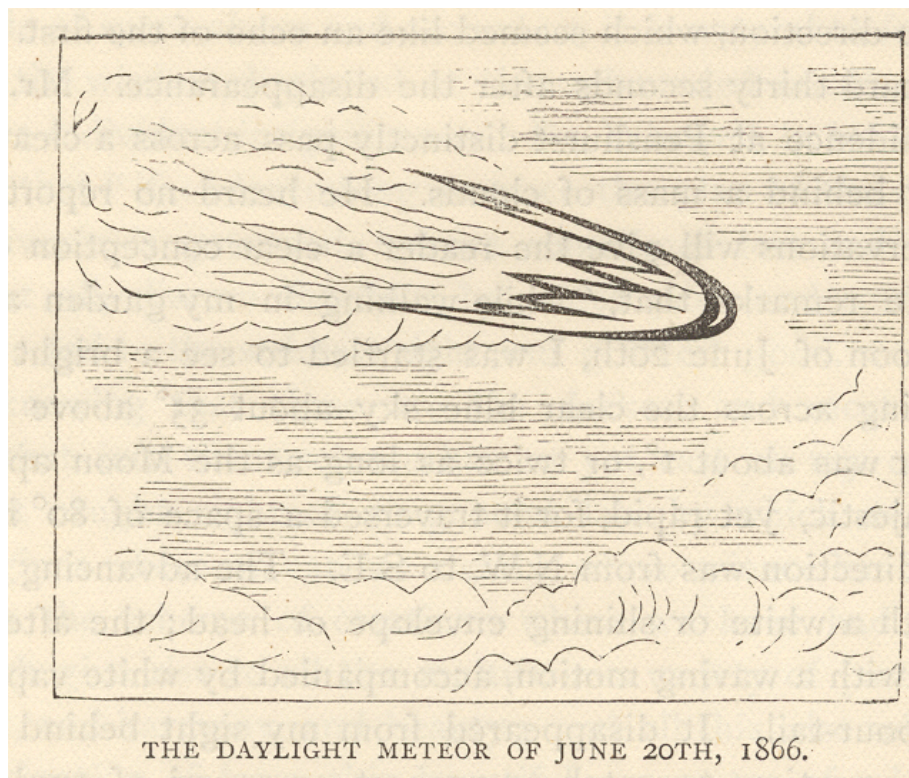
## The daylight meteor of 1866 June 20

*Chris Trayner*

---

A brief description of a nineteenth-century bolide is given. Contemporary accounts and a picture are presented.

---



Fireballs are unpredictable events, and networks of cameras have been set up to record them reliably. Before these networks were set up there were occasional high-quality records of fireballs, however. This short historical note records one such from 1866. These details come from (Dunkin, 1880), as does the illustration above, which sadly is without attribution or further details.

The bolide ‘appeared about a quarter to eleven on the morning of June 20th, 1866, and was visible as a very brilliant object from various parts of England and the continent, principally, however, in the counties of Kent and Sussex, at Boulogne, Calais, and Lille, in France, and as far away as Delft in Holland. [It probably] exploded over some part of the district between the towns of Boulogne and St. Omer.’ (ibid.)

Nasmyth saw it and recorded a pleasingly professional description, quoted in the same book. ‘While walking in my garden at about a quarter to eleven on the forenoon of June 20th, I was startled to see a bright red comet-shaped object rapidly moving across the clear blue sky about 35° above the horizon. The length of the meteor was about 1°, or twice as long as the Moon appears in diameter. The motion was majestic, yet rapid, for it traversed a space of 80° in rather less than two

seconds. The direction was from N.W. to S.E. The advancing end of the meteor was brilliant red, with a white or shining envelope or head ; the after part, or tail, was a ragged fan-shape, with a waving motion, accompanied by white vapours, and followed by a faint white vapour-trail. It disappeared from my sight behind a mass of clouds, and I listened for some time to catch any report or sound of explosion, but I heard none. The passage of the meteor was nearly parallel to the horizon, but with a slight dip or decline to the S.E. It is impossible to convey by words the impression left by the appearance of this mysterious object, majestically traversing the clear blue sky during bright sunshine. Had it made its appearance at night, the whole of England would have seen more or less of its light.’ (ibid.)

Dunkin is frustrating in his lack of proper references. He merely refers to the author of this quote as ‘Mr. Nasmyth’. It is presumably James Nasmyth (1808–90), a renowned engineer and amateur astronomer, and inventor of the Nasmyth focus for telescopes.

### References

Dunkin, Edward (c.1879–80) “The Midnight Sky (New and Revised Edition)”, The Religious Tract Society, London, 333–334.

# The International Meteor Organization

web site <http://www.imo.net>

## Council

*President:* Jürgen Rendtel,  
Eschenweg 16, D-14476 Marquardt, Germany.  
tel. +49 33208 50753  
e-mail: [jrendtel@aip.de](mailto:jrendtel@aip.de)

*Vice-President* Alastair McBeath  
12A Prior's Walk, Morpeth,  
Northumberland NE61 2RF, UK.  
tel. +44 1670 518487  
e-mail: [meteor@popastro.com](mailto:meteor@popastro.com)

*Secretary-General:* Robert Lunsford  
161 Vance Street, Chula Vista,  
CA 91910-4828, USA. tel. +1 619 585 9642  
e-mail: [lunro.imo.usa@cox.net](mailto:lunro.imo.usa@cox.net)

*Treasurer:* Ina Rendtel  
Mehlbeerenweg 5, D-14469 Potsdam, Germany  
tel. +49 331 520 707  
e-mail: [IRendtel@t-online.de](mailto:IRendtel@t-online.de)  
Postal (giro) account number: 5472 34-107  
Bank code: 100 100 10 Postbank Berlin  
(When paying, state bank code and postbank  
as well as account number!)

*Other council members:*  
Rainer Arlt, Friedenstraße 5, D-14109 Berlin,  
Germany. e-mail: [rarlt@aip.de](mailto:rarlt@aip.de)  
David Asher, Armagh Observatory, College Hill,  
Armagh BT61 9DG, Northern Ireland, UK.

e-mail: [dja@star.arm.ac.uk](mailto:dja@star.arm.ac.uk)  
Malcolm Currie, 25, Collett Way, Grove,  
Wantage, Oxfordshire OX12 0NT, UK.  
e-mail: [mjc@star.rl.ac.uk](mailto:mjc@star.rl.ac.uk)  
Marc Gyssens, Heerbaan 74, B-2530 Boechout,  
Belgium. e-mail: [marc.gyssens@luc.ac.be](mailto:marc.gyssens@luc.ac.be)  
André Knöfel, Habichstraße 1,  
D-15526 Reichenwalde, Germany.  
e-mail: [aknoefel@minorplanets.de](mailto:aknoefel@minorplanets.de)  
Sirko Molau, Abendstalstraße 13b,  
D-84072 Seysdorf, Germany.  
e-mail: [sirko@molau.de](mailto:sirko@molau.de)  
Mihaela Triglav-Čekada, Streliška 9,  
SI-1000 Ljubljana, Slovenia.  
e-mail: [mtriglav@yahoo.com](mailto:mtriglav@yahoo.com)

## Commission Directors

*Fireball Data Center:* André Knöfel  
*Photographic Commission:* Marc de Lignie  
Steve Bikostraat 298,  
NL-3573 BH Utrecht, The Netherlands  
e-mail: [m.c.delignie@xs4all.nl](mailto:m.c.delignie@xs4all.nl)  
*Radio Commission:* vacant  
*Telescopic Commission:* M. Currie  
*Video Commission:* Sirko Molau  
*Visual Commission:* Rainer Arlt

## WGN

*Editor:* Chris Trayner  
32 Moor Park Villas, Leeds LS6 4BZ, UK  
fax: +44 113 3432032; mark "for C. Trayner"  
tel: +44 113 2302687 e-mail: [wgn@imo.net](mailto:wgn@imo.net) ;  
include METEOR in the e-mail subject line  
*Editorial board:* R. Arlt, M. Gyssens,

A. McBeath, J. Rendtel, M. Triglav-Čekada.  
*Advisory board:* D.J. Asher, M. Beech, P. Brown,  
M. Currie, M. de Lignie, W.G. Elford,  
R.L. Hawkes, D.W. Hughes, J. Jones, C. Keay,  
G.W. Kronk, R.H. McNaught, P. Pravec,  
G. Spalding, M. Šimek, I. Williams.

## IMO Sales

*Available from the Treasurer*

**Proceedings of the International Meteor Conference**  
1990–1996  
1997  
1998–2000, 2002–2003  
2001 — on CD only

€	\$
5	5
Out of print	
6	6
5	5

### Back issues of WGN

Vols. 19–22 (1991–1994) per complete volume	10	10
Vols. 23–29 (1995–2001) per complete volume	18	18
Vol. 30 (2002) per complete volume	20	20

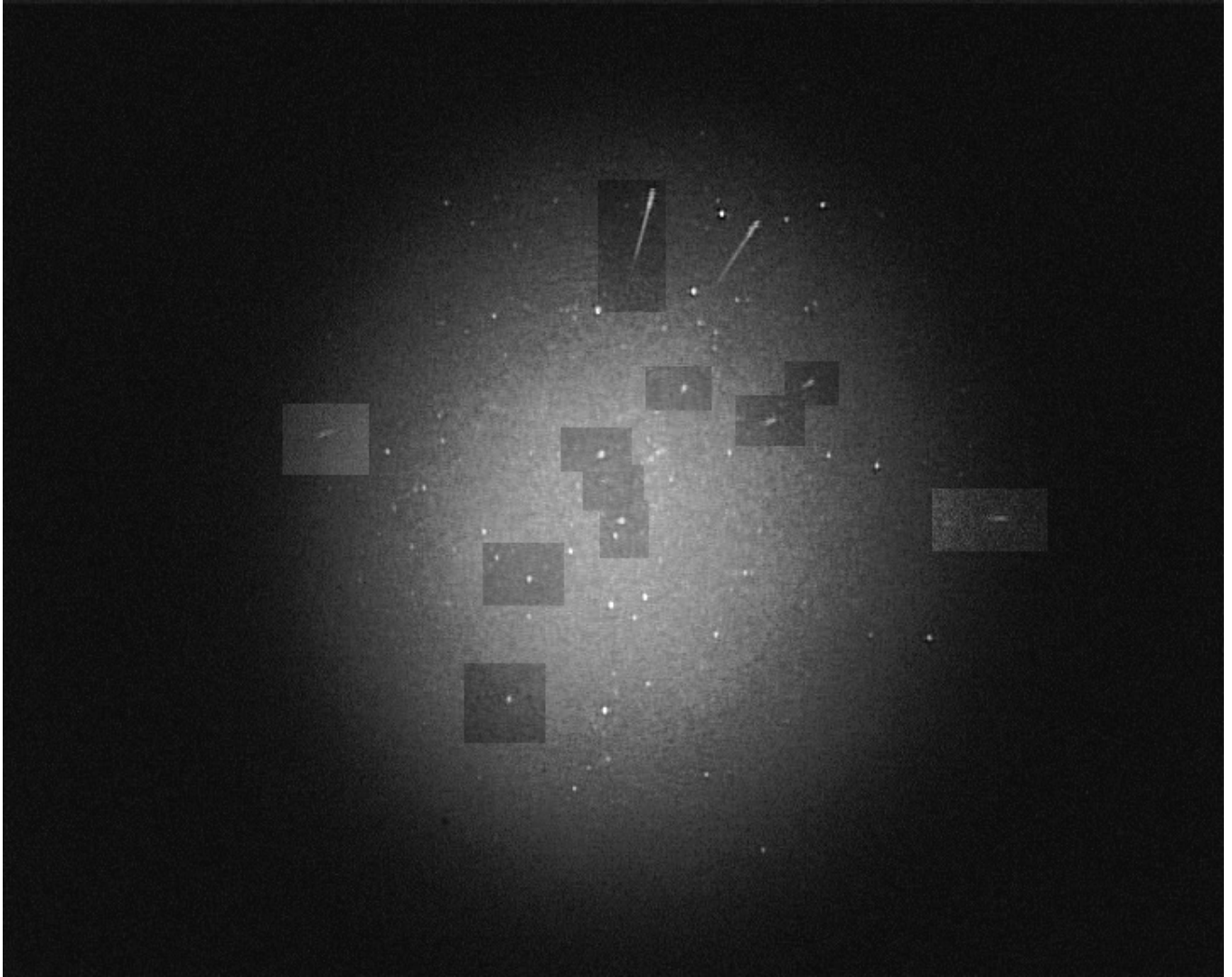
### WGN Observational Report Series

Vols. 1–5 (1988–1992) Visual Observations, per volume	8	8
Vol. 6 (1993) Visual Observations and Electrophonic Fireball Catalogue	8	8
Vols. 7–8 (1994–1995) Visual Observations, per volume	8	8
Vols. 9–14 (1996–2002) Visual Observations, per volume	10	10

### Other publications

Photographic Meteor Database (1986)	4	4
Photographic Astrometry + diskette	7	7

# Perseids 2004



Montage of twelve Perseids recorded on video on 2004 August 11, between 21<sup>h</sup>00<sup>m</sup> and 21<sup>h</sup>10<sup>m</sup> UT.

Intensifier: 'Delnocta' first generation 3-traps intensifier from 'Olde Delft Instruments'.

Camera: Sony DCR-TRV900E PAL (720 × 576 pixel) camera in black & white mode.

Lens: Sony V-mount  $f = 25$  mm,  $f/2.8$ , field of view 35°.

From every meteor one frame was pasted into a total view of the video to give an impression of the event.

Observations from Britzingen, Germany, by Carl Johannink, Koen Miskotte, Romke Schievink and Rita Verhoef. Video processing by Romke Schievink.